A Contribution to the Development of High-Voltage dc Circuit Breaker Technologies
A Review of New Considerations

Liu, Zhou; Mirhosseini, Seyed; Liu, Lian; Popov, Marjan; Ma, Kaiqi; Hu, Weihao; Jamali, Sadegh; Palensky, Peter; Chen, Zhe

DOI
10.1109/MIE.2021.3085998

Publication date
2022

Document Version
Final published version

Published in
IEEE Industrial Electronics Magazine

Citation (APA)
Liu, Z., Mirhosseini, S., Liu, L., Popov, M., Ma, K., Hu, W., Jamali, S., Palensky, P., & Chen, Z. (2022). A Contribution to the Development of High-Voltage dc Circuit Breaker Technologies: A Review of New Considerations. *IEEE Industrial Electronics Magazine*, *16*(1), 42-59. https://doi.org/10.1109/MIE.2021.3085998

A Contribution to the Development of High-Voltage dc Circuit Breaker Technologies

A Review of New Considerations

ZHOU LIU, SEYED SATTAR MIRHOSSEINI, LIAN LIU, MARJAN POPOV, KAIQI MA, WEIHAO HU, SADEGH JAMALI, PETER PALENSKY, and ZHE CHEN

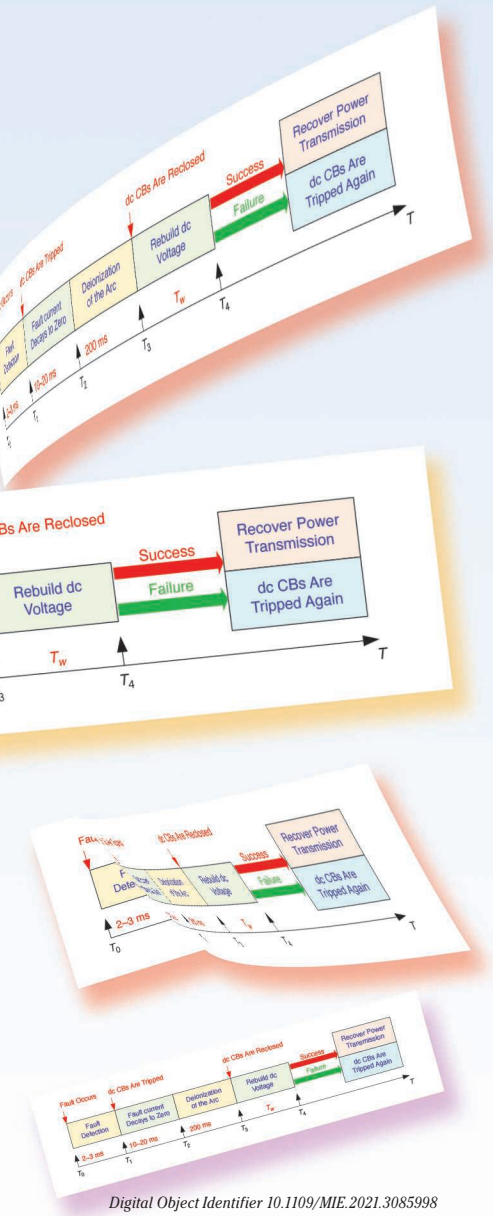

Digital Object Identifier 10.1109/MIE.2021.3085998
Date of current version: 15 July 2021

To promote the integration of renewable energy resources into modern energy systems, high-voltage dc (HVdc) and circuit breaker (CB) technologies have become critical to achieving secure and efficient energy transmission. This article reviews the technical development of the related areas, compares diverse breaker concepts and topologies, investigates possible coordination and testing solutions, and points out the remaining challenges as well as future needs. The time-domain simulation and comparative analysis are adopted in this article to analyze and compare the performances of different HVdc CBs. By making use of different selectivity levels of multiterminal HVdc (MTdc) grids, the suitable planning and placement of HVdc CBs can be conducted. Furthermore, by providing insights into the performance of HVdc CBs, the work presented in this article can serve as a useful asset for the upcoming standardization and industrial application process of HVdc grid and CB design and testing.

Introduction

Today, it is a common trend in power systems to exploit renewable energy resources instead of traditional fossil fuels as they have more advantages related to the environment as well as an inexhaustible energy cycle [1]. To help integrate and transfer a large amount of renewable energy resources, especially those from diverse onshore and offshore sites, the development of the MTdc grid has become an emerging demand. Some relevant leading projects have been commissioned or are being developed, e.g., the Québec–New England three-terminal HVdc system [2], the Nan'ao four-terminal HVdc system [3], and the Zhou Shan five-terminal grid [4].

The main challenge when implementing MTdc grids is the vulnerability of such grids resulting from dc

1932-4529/22©2022IEEE

short circuit faults [5]. Due to their fast dc current rise, the outages caused by such severe disturbances can easily propagate from one converter station to another. Thus, a dc CB is of vital importance to making the MTdc grid secure and to paving the way toward the integration of a bulk amount of offshore wind power to the ac grid to ensuring the system's high efficiency, reliability, and controllability [6], [7]. Until now, dc CBs have been widely available for application in the medium- and low-dc-voltage levels [8]. Because of the high requirements on fault detection, fault current interruption, and energy dissipation in HVdc systems, the most important challenges to realizing MTdc grids are dc CBs and dc protection.

The timeline for the development of dc CBs is shown in Figure 1. As we know, Thomas Edison is regarded as an originator on the development of the dc power system, and dc technology could have existed even earlier [10]. Along with the development of HVdc systems, the research on dc CBs commenced in the 1940s, which was earlier than the commissioning of the first commercial HVdc transmission link in 1954 [11]. From the 1940s to the 1980s, line-commutated converter (LCC) HVdc systems evolved from mercury arc valve-based HVdc systems to thyristor-based ones (born in the 1970s); and with high interest in MTdc grids in the 1980s, a lot of research on dc CBs was subsequently conducted [12]. As one of the most important achievements, Hitachi successfully tested a 250-kV/8-kA mechanical HVdc CB in 1985 [13]. In 1988, another mechanical HVdc CB, with the rating of 500 kV/4 kA, was tested by the Brown Boveri Company, the Electric Power Research Institute, and the Bonneville Power Administration [14]. Although, as seen in Figure 1, the interest in HVdc CBs declined after 1988, it arose again, thanks to the emerging voltage source converter (VSC) HVdc systems that resulted from the development of VSC and modular multilevel converters (MMCs) in 1997 and 2003, respectively [15], [16]. The fault-interrupting speed of the breakers used in LCC HVdc systems is much lower than that of the minimum requirement of VSC HVdc systems.

In 2011, the successful testing of a 320-kV/16-kA ABB hybrid HVdc CB was performed [17]. A 200-kV/15-kA hybrid dc CB consisting of cascaded full-bridge insulated-gate bipolar transistor (IGBT) submodules was installed in the Zhoushan MTdc grid [18] in 2016, and a 500-kV hybrid dc CB with a similar structure is soon to be deployed in the Zhangbei MTdc grid. In 2018, the world's first 160-kV/9-kA mechanical HVdc CB was utilized in the China southern Nan'ao MTdc power grid [9]. A 160-kV/16-kA Mitsubishi Electric mechanical HVdc CB was successfully tested in 2019 [19]. In 2020, successful testing was performed on an 80-kV/15-kA SCiBreak, VSC-assisted, resonant current HVdc CB [20]. Until now, many publications and reports have addressed only a few aspects of the requirements of dc CBs in MTdc grids, while this article provides an overall picture of dc CB technologies in terms of the challenges, requirements, time-domain simulation, cost, and testing considerations.

Placement, Challenges, and Requirements of dc CBs in MTdc Grids

Dc CB Placement and Fault-Clearing Strategies

The dc CB placement and implementation of the related protection schemes is tightly related to the converter types, which determine the features of fault current flowing through HVdc systems. There are three basic converter topologies: LCCs, two- or three-level VSCs, and MMCs [21]. A novel concept, based on the diode rectifier unit as an offshore converter for offshore wind farm integration [22], belongs to a special case of LCCs. As the LCC and two- and three-level technologies have some limitations, the MMC technology is commonly accepted as a suitable solution for MTdc grids [23]. Two basic types of MMCs can be easily defined: 1) the nonfault interruption type, i.e., an MMC with half-bridge submodules, and 2) the fault interruption type, i.e., an MMC with full-bridge submodules.

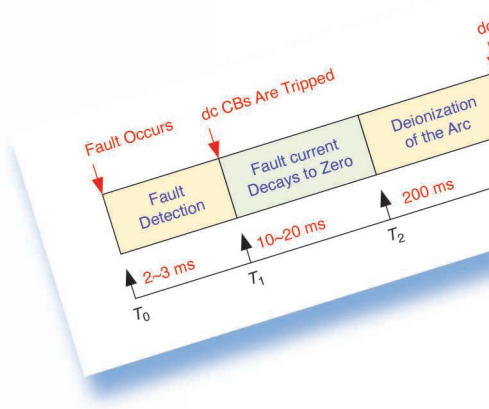

According to the CIGRÉ Technique Brochure 739 [24], three types of fault-clearing strategies (FCSs), including nonselective and partially and fully selective strategies, can be considered for an MTdc grid. These strategies are defined in Table 1, together with examples, considering the MTdc grid presented in Figure 2 [25]. The ac CBs are installed between the half-bridge converter terminals and ac grid, and the dc disconnectors are located in the place that isolates the faulty part in the MTdc grid. This is the traditional protection method that normally leads to the outage of the whole dc system [26]. To avoid a power loss in the whole system, a full-bridge MMC with a fault interruption function can be adopted, which could suppress the dc-side fault current by isolating the fault injection from the ac side [27]. Moreover, by using a dc CB, the faulted sections in MTdc grids could be quickly isolated in a similar way as an ac CB does in the ac grids, which provides better selectivity upon dc fault clearance [28]. With dc CBs, no special topologies are required for the MMCs, but different control strategies may need to be developed for different MMC types during the faults. Mixed methods could be defined, which for future applications are also likely to provide hierarchical protection with more reliability and much faster restoration capability [29].

It can be seen that dc CBs need to be placed at the remote ends of the lines and at each side of the nodes for the fully selective FCS, which makes the cost very high. In contrast, the cost will be lowest when the nonselective FCSs are applied with fewer

dc CBs. And in the middle, the whole grid can be split into subgrids (e.g., the two gray circles in Figure 2) with several dc CBs installed at the borders of these subgrids when the partially selective FCS is applied [25]. Based on the aforementioned discussions, it can be seen that investment costs of the dc fault clearance are influenced by the method of the dc fault current interruption and the selectivity level of protection strategy.

Dc CB Challenges

Dc Fault Analysis

Prior to addressing dc CB challenges, the related dc fault current analysis in an MTdc grid is of significance. To analyze the dc fault current, a pole-to-ground fault is applied on the cable between terminals 2 and 3 in the bipole half-bridge MMC-based MTdc grid in Figure 2 with a voltage level of ±320 kV [30]. The fault-transient progress can be divided into three stages, which can be observed in Figure 3 [24], [25], [30], [31]. Iconverter, Iline.fault, and Iline.unfault represent the converter output current at terminal 2, the currents flowing through the faulty line, and the unfaulty line between terminals 1 and 2, respectively.

After the fault occurs, at instant t_1, traveling waves arrive at MMC terminal 2 through the faulted line end of the dc reactor, which partly initiate

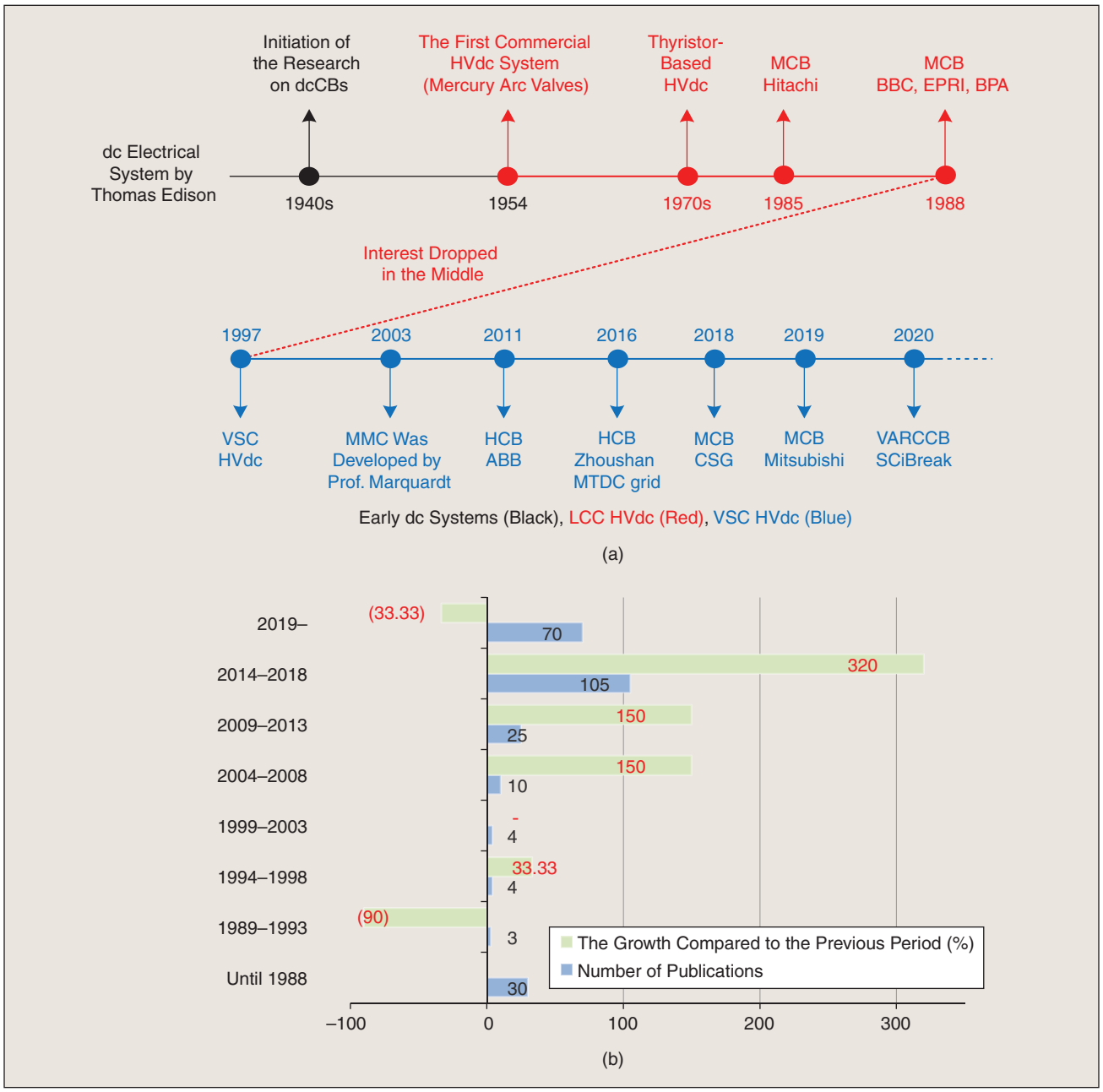

FIGURE 1 — (a) The timeline for the development of dc CBs and (b) the general number of publications on HVdc CBs. MCB: mechanical CB; HCB: hybrid CB; VARCCB: VSC-assisted resonant current CB; MMC: modular multilevel converter; VSC: voltage source converter; CSG: China southern grid; LCC: line-commutated converter; ABB: Asea Brown Boveri Ltd; EPRI: Electric Power Research Institute; BBC: Brown Boveri Company; BPA: Bonneville Power Administration.

the submodule discharging and then result in a fast current increase. The converter can still keep its control of the ac-side voltages and currents to support the dc fault current rise until the arm currents violate the threshold of the converter blocking at t_2. Because the neighboring line connected to terminal 2 discharges, the current flowing through the faulty line (Iline.fault) rises at a slightly higher rate than that of the Iconverter. After the converter blocks at t_2, the submodule capacitors are bypassed by freewheeling diodes. Hereby, the capacitor discharge is interrupted and the converter cannot keep the control of the ac sides. As there is no inherent voltage support, only the arm reactors keep the current flowing through the diodes. Thus, during stage 2, the dc current of the converter decays until the ac infeed starts at t_3. When the arm currents decay to zero at t_3, the converter is changed to a diode rectifier operation mode, then the dc current results from the ac infeed, i.e., Iconverter becomes only Iac.infeed.

Assuming that the dc CBs and ac CBs have still not interrupted the fault, Iline.fault has a higher value than that of Iconverter due to the infeed from the neighboring line (Iline.unfault). The related general equivalent circuits of stages 1 and 3 are listed in Table 2 [24], [30], [31]. At stage 2, only the arm currents decaying through the arm reactors and diodes are included. The analytical expression of the instantaneous fault current and its rate of rise at stage 1 are given by (1) and (2) while the average dc current in the rectifier operation mode at stage 3 is expressed by (3).

From this analysis of the dc fault current in the MTdc grids, it can be seen that the dc parameters will mainly define and influence the transient fault current at stage 1, and the steady-state fault current at stage 3 is related to both the ac- and dc-side parameters. The dc fault characteristics with a high rate of rise of the fault current and without a current zero crossing define the requirements and challenges of the dc CB design, which are very different from those in an ac system. Also, creating a current zero in the normal current path for a timely fault current interruption is the primary consideration of the dc CB designs, which is not an issue in the design of ac CBs.

Comparisons and Challenges

For both ac and dc CBs, three operation stages can be defined: 1) the breaker opening or current commutation, 2) the arcing and energy dissipation, and

TABLE 1 — THE MAIN FCSs.

FCSs IN MTdc GRIDS		EXAMPLES (THE MTdc GRIDS AND THEIR RELATED COMPONENTS ARE DEPICTED IN FIGURE 2)
Nonselective	The dc grid is regarded as one protection zone.	The dc fault F1 is cleared by only the red elements in the grid, i.e., ac CBs or full-bridge converters or dc CBs behind the converter terminals.
Partially selective	The dc grid is split into subgrids, i.e., several protection zones.	Two subgrids are formed with an insufficient dc CB installation, and F1 is cleared by dc CB4 and dc CB6, which are installed at the border of the subgrids.
Fully selective	Each dc branch and node are defined as *protection zones*.	With a sufficient dc CB installation, the fault element is disconnected by the dc CBs at both ends of the element, e.g., F1 is cleared by dc CB4 and dc CB5.

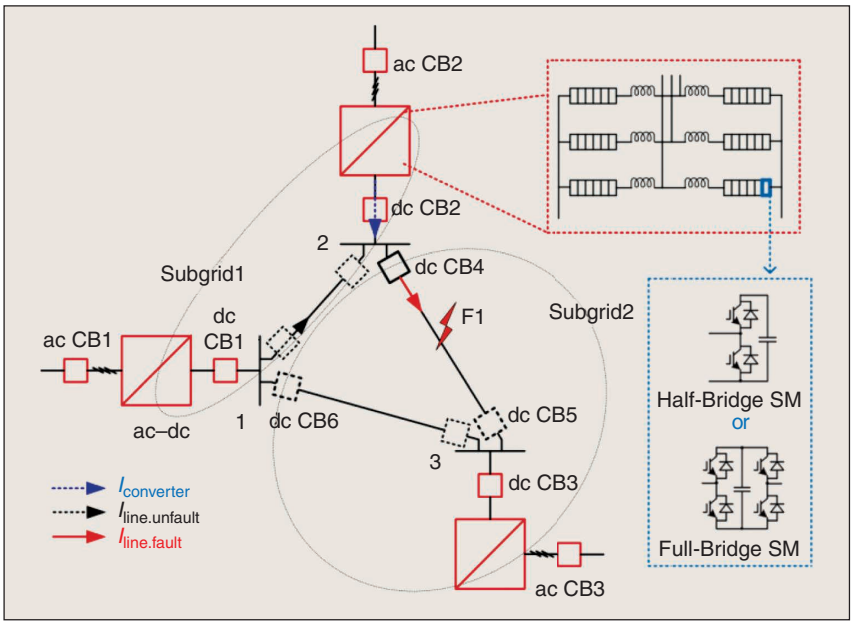

FIGURE 2 — A simple MTdc grid protected by different FCSs. SM: submodule.

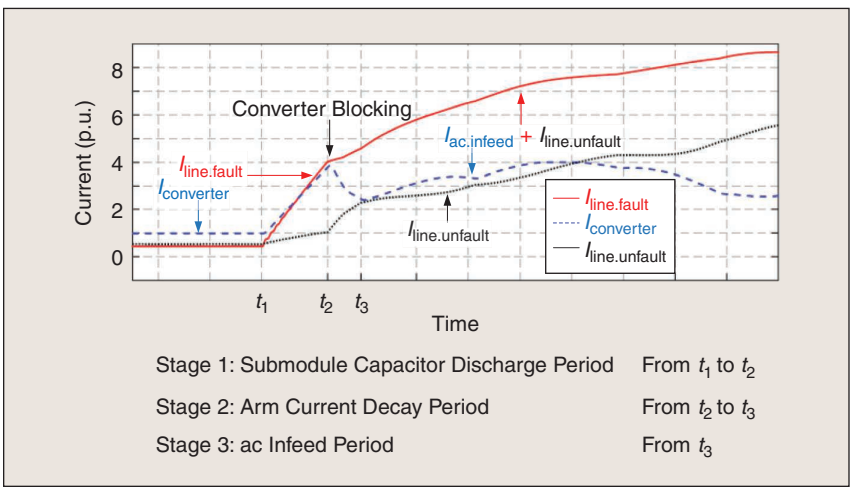

FIGURE 3 — The development progress and the stages of dc short circuit currents. p.u.: per unit.

3) fault interruption [25]. However, in MTdc grids, dc fault currents are normally characterized by a high rate of rise and the absence of natural current zero crossing points. Due to this high increasing rate, the limitation of the fault-clearing time becomes a challenge, which demands a fast breaker to interrupt the fault current before it rises to uncontrollable levels [32]. The value of the prospective steady-state fault current is mainly determined by the ac network strength, and the increase of the dc-side inductance will decrease the rate of rise of the dc fault current [33]. These two factors give rise to the requirements and constraints on the selection of the FCS and the related dc CB applications. Moreover, the maximum power loss due to a dc fault and the transient-stability limits of an ac network should be considered, which provides time-related constraints for the dc fault clearance [34]. And the fault-clearing times are normally defined in the order of tens of milliseconds, which are regarded as the maximum allowable clearing time, concerning the power system's transient stability [24]. The need for shorter clearing times, however, ranging from 2 to 5 ms, are reported in [5].

Another challenge for dc CB technology originates from the second characteristic of dc fault currents, i.e., the additional branches are required to help the interruption of the dc fault currents at artificial zero crossing points by absorbing the energy stored in the grid. Interrupting the normal load branch current is realized by commutating the current to the additional branches, which imposes HV stress across the dc CB. This HV stress results in challenges in design considerations for the normal load branch and the additional branches, mainly in terms of insulation strength and the short time required for current commutation. Moreover, during the fault-current-suppression period, dc CBs should withstand an HV and a high current at the same time, which is equal to the large amount of energy required to be absorbed by one of the additional branches [12], [17]. Due to the different mechanism and the development status of the ac and dc CBs in an HV system, a brief comparison can be seen from the aspects of the breaking current, the interruption time, the reclosing, the production, and the standardization in Table 3 [25], [35]–[38].

Operational Requirements for dc CBs in MTdc Grids

Based on the aforementioned discussions, the operational requirements can be derived as follows.

- the capability to create current zeros and to reliably interrupt the possible maximum fault current in an MTdc grid
- a shorter clearing time; the total fault-clearing time is expected to be shorter than 20 ms, which is associated with the lowest timescales in transient-stability limits of connected ac system [34].
- energy dissipation capability, which should be sufficient to timely dissipate the energy stored during faults
- the capability to withstand the transient impulse voltage after current interruption
- reliable backup protection for breaker failure, which is significant to activate backup breakers with

TABLE 2 — THE GENERAL EQUIVALENT CIRCUITS AND ANALYTICAL EXPRESSIONS OF FAULT CURRENTS IN STAGES [24], [30], [31].

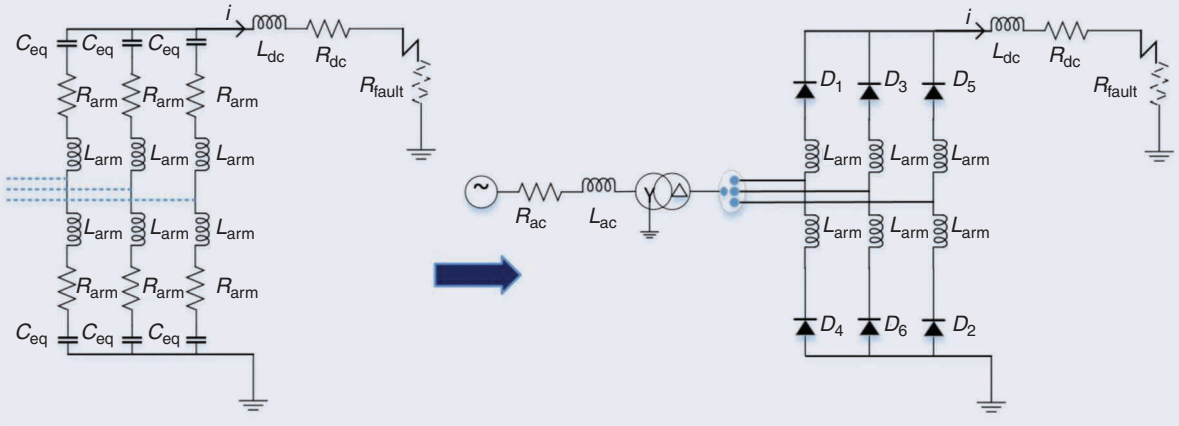

Stage 1: Submodule Capacitor Discharge Period

Stage 3: ac Infeed Period

$$i(t) = [(Bw - A\alpha)\cos(wt) - (Aw + B\alpha)\sin(wt)]\exp(-\alpha t) \quad (1)$$

$$\frac{di}{dt} = [B(w^2 + \alpha^2)\sin(wt) - A(w^2 - \alpha^2)\cos(wt)]\exp(-\alpha t) \quad (2)$$

where $\alpha = \frac{R}{2L}$, $w = \sqrt{\frac{dy}{dx} - \left(\frac{R}{2L}\right)^2}$, $A = CV_{dc}$, $B = \frac{I_0 + A\alpha}{w}$

$$R = R_{dc} + R_{fault} + \frac{2}{3}R_{arm},\ L = L_{dc} + L_{calbe} + \frac{2}{3}L_{arm},\ C = 6C_{eq}$$

$$I_{ac,\,component} = \frac{\frac{2}{\pi}\sqrt{2}\,V_{ac}}{Z_{total}} \quad (3)$$

where $Z_{total} = Z_{ac} + Z_{tr} + \frac{1}{2}Z_{arm} + \frac{2}{3}(Z_{dc} + R_{fault})$,

Z_{ac}: ac system impedance
Z_{tr}: converter transformer impedance
Z_{dc}: dc-side impedance
Z_{arm}: converter arms impedance

a reasonable current interruption capability.
- proper coordination among the protection schemes, converter controls, and dc CBs, especially in case of a breaker failure.

Positioning of dc CB Technologies

General Categories of dc CBs

Compared to ac CBs, dc CBs need to be modified with additional branches (i.e., commutation and energy-dissipating branches) to create a current zero crossing or to enforce the dc fault current to zero during current interruption [39], which can be observed in Figure 4. According to the different types of dc CBs, the mechanism of the commutation branch will be different, and the current interruption could occur in a different branch, i.e., the nominal current or commutation branch. As a dc CB needs to withstand both HV and high current [i.e., transient interruption voltage (TIV) and peak fault current] during the fault-current-suppression period, an energy-dissipating branch is required to absorb the fault current and to dissipate the energy stored during the interruption process. A typical interruption process of a mechanical CB (MCB) is shown in Figure 4(b) and (c) [7].

TABLE 3 — A COMPARISON BETWEEN ac CB AND dc CB IN HV SYSTEMS.

	ac CB	dc CB
Related break current	• 40/50/63 kA at the related voltage of 362/500/800 kV	• up to approximately 25 kA at 320 kV
The breaking time	• two or three cycles (50/60 Hz) for voltages below 362 kV • 33 ms for voltages above 500 kV	• roughly 2 ms to interrupt fault currents up to approximately 25 kA in 320-kV HVdc systems
Reclosing requirement and the time required	• the standard operation sequence is O-t-CO-t′-CO, where O represents open, CO is close-open, and t is the reclosing time	• dc CB at the healthy lines under nonselective protection • for backup operation • as primary protection for overhead lines for the self-clearing faults with fully selective protection • rapid reclosing might be required for the aforementioned situations
	• normal reclosing time: 3 min • rapid reclosing time: 0.3 s	• reclosing times are to be defined in the different HVdc systems
Production	• single-vendor oriented	• multiple-vendor oriented
Standardization	• well-established methods for testing, e.g., IEEE c37.06 and IEC 60255	• no standards for dc grid protection and dc CB

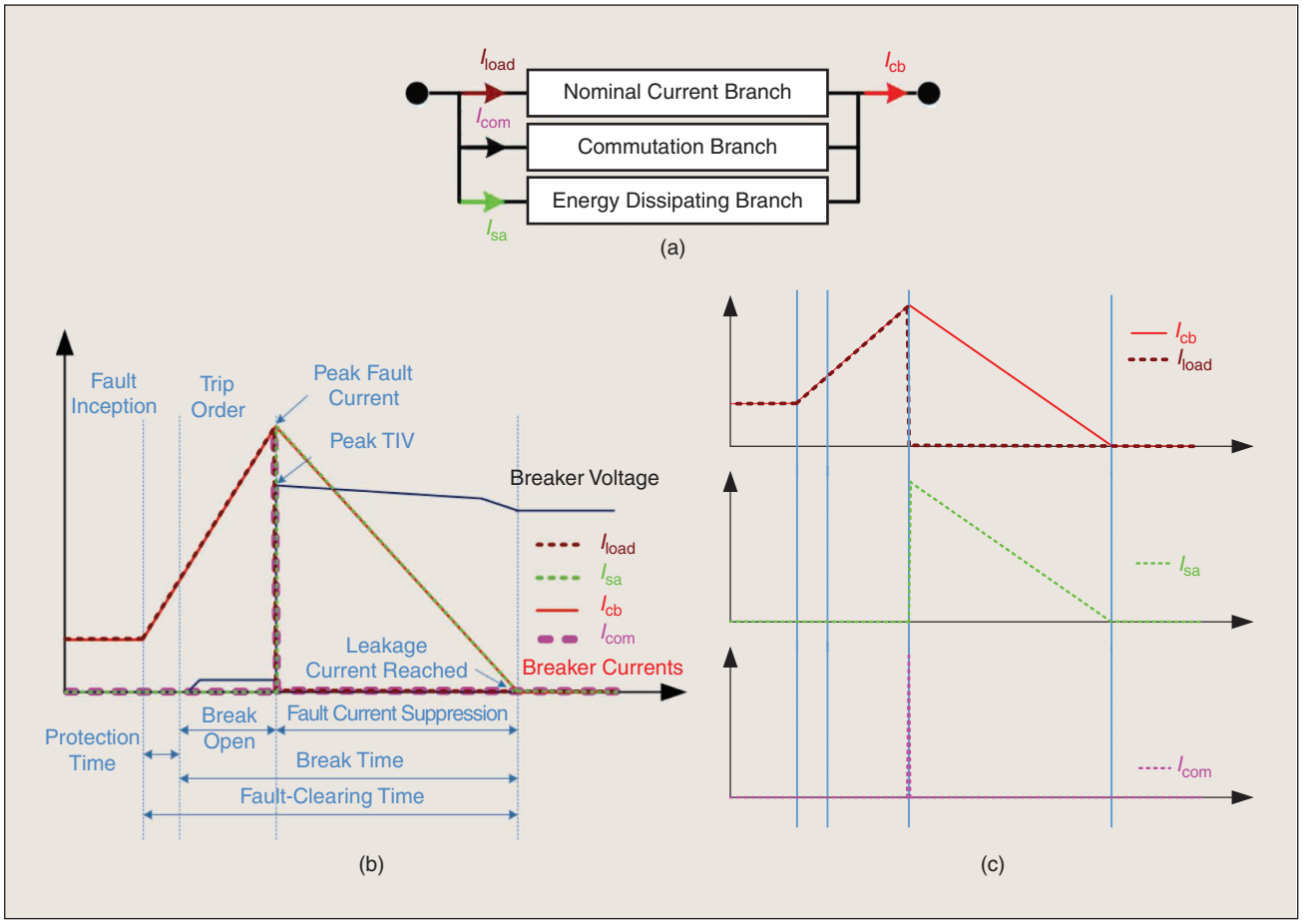

FIGURE 4 — (a) A generic dc CB model, (b) the dc CB interruption progress, and (c) the breaker currents.

Recent Developments

There are four main types of dc CBs mentioned in the literature: MCBs, VSC-assisted resonant current CBs (VARCCBs), HCBs, and SSCBs [5].

MCBs

In [39], MCBs are classified as passive- and active-resonance CBs. The precharged capacitor is normally used in the active-resonance circuit (in the commutation branch) to create active oscillations instead of self-excited growing oscillations [40]. Different categories can be also made based on the diverse structures and interrupter types. The configuration of a typical active-resonance MCB is displayed in Figure 5(a). In this MCB, the main branch is composed of a mechanical interrupter [that is, a vacuum interrupter (VI)] and a residual current breaker (RCB). The interrupter can be an oil breaker [41], air-blast breaker [42], VI [43], or SF_6 gas breaker [44]. The interrupter is actuated by an ultrafast mechanical mechanism, such as a Thomson-coil mechanism to rapidly provide a sufficient contact-gap distance, thus ensuring an adequate dielectric strength for the VI so that it can endure the TIV.

The current injection branch is composed of a resonance circuit, including a capacitor (Cp) and an inductor (Lp) in series with an injection switch (S_3). A surge arrester (SA) is connected across Cp and S_3 as an energy-dissipating branch. During the current interruption, a short time after receiving the trip order, the VI opens and the arc current passes through the VI. At the same instant, S_3 closes and the precharged resonance circuit injects an oscillating current for creating current zeros in the main branch, which provides the appropriate conditions for vacuum interruption. By interrupting the current in VI in one of the artificial current zero points, the breaker current is transferred to the injection circuit for a very short time, which makes the voltage across the SA increase up to its clamping voltage. The current is commutated to the energy-dissipating branch. By absorbing the energy into the SA, the current decreases toward zero and the RCB opens to interrupt the residual current passing through the MCB.

The whole breaker can be made by one single breaker unit or be the series connection of several individual units with a lower voltage rating [13]. In classical MCBs, arc features under different conditions and the parameter optimization of critical capacitors and varistors become important research targets [45], [46]. The requirement for fast interruption is challenging for medium-voltage and HV breakers, even with active current injection circuits and VI [32]. Recent developments on active current injection MCBs demonstrates a 5–10-ms breaking time and an interruption capability of up to 16 kA [38], [48].

VARCCBs

The configuration of the VARCCB, which can be considered a novel type of an active-resonance mechanical dc CB, is illustrated in Figure 5(b). Similar to an MCB, the main branch is composed of a VI, which is actuated by an ultrafast Thomson-coil mechanism, and an RCB. The dissipating branch is composed of an SA. The current injection branch (i.e., the commutation branch) consists of two parts: 1) a resonance circuit composed of a resistor (Rp), a capacitor (C_p), and an inductor (L_p) and 2) a VSC composed of four IGBTs, an energy storage capacitor (C_{DC}), and a charging circuit (V_{DC} and R_{CH}). By changing its output voltage polarity in the same direction as that of the oscillating injection current, the VSC quickly increases the amplitude of the oscillating current. The branch capacitor (C_p) in the VARCCB is not precharged, which, by contrast, is precharged in the MCB, and the VSC energy storage capacitor (C_{DC}) is precharged. The current interruption process of the VARCCB is similar to that of the MCB. The main difference is that the amplitude of the oscillating injection current increases by means of the VSC. Therefore, the VARCCB can reach a shorter breaking time. A recent development on the VARCCB reports a 2–8-ms breaking time and an interruption capability of up to 16 kA. Depending on the rated voltage, the VARCCB may also be a single unit or consist of the series connection of several individual units [49], [50].

Hybrid CBs

The classical configuration of the HCB can be observed in Figure 5(c) [40]. When a fault occurs, the trip order arrives at the dc CB, and then the load current switch (LCS) in the normal load branch turns off. The main dc breaker (MB) turns on at the same time, and then the current is transferred from the normal load branch to the main breaker branch. The ultrafast disconnector (UFD) starts to open when the current is totally transferred to the main breaker branch. The MB is turned off when the UFD is fully opened and the current is commutated to the energy-dissipating branch. The current decreases toward zero by absorbing the energy in the SA, and finally, the RCB opens to interrupt the residual current passing through the HCB.

It should be noted that here, only system-level, simplified dc CB models are presented to deal with general performances, and the component-level dc CB models with detailed internal components are not presented, e.g., the cascaded submodules of IGBTs in the branches, as described in [40]. As the rating of the most powerful IGBTs is in the order of a few kilovolts and kiloamperes to withstand the TIV and the fault current in MTdc grids, the main breaker branch includes several series- and parallel-connected IGBT modules. The required number of series IGBT modules depends on the rated voltage, while the required number of parallel IGBT modules is determined by the current interruption capability of the dc CB. As the normal load branch is not exposed to high voltages and currents, its required number of series and parallel IGBT modules is lower than that of the main breaker branch.

To ensure equal voltage distribution during current interruption, a snubber circuit needs to be installed across each IGBT module. To be

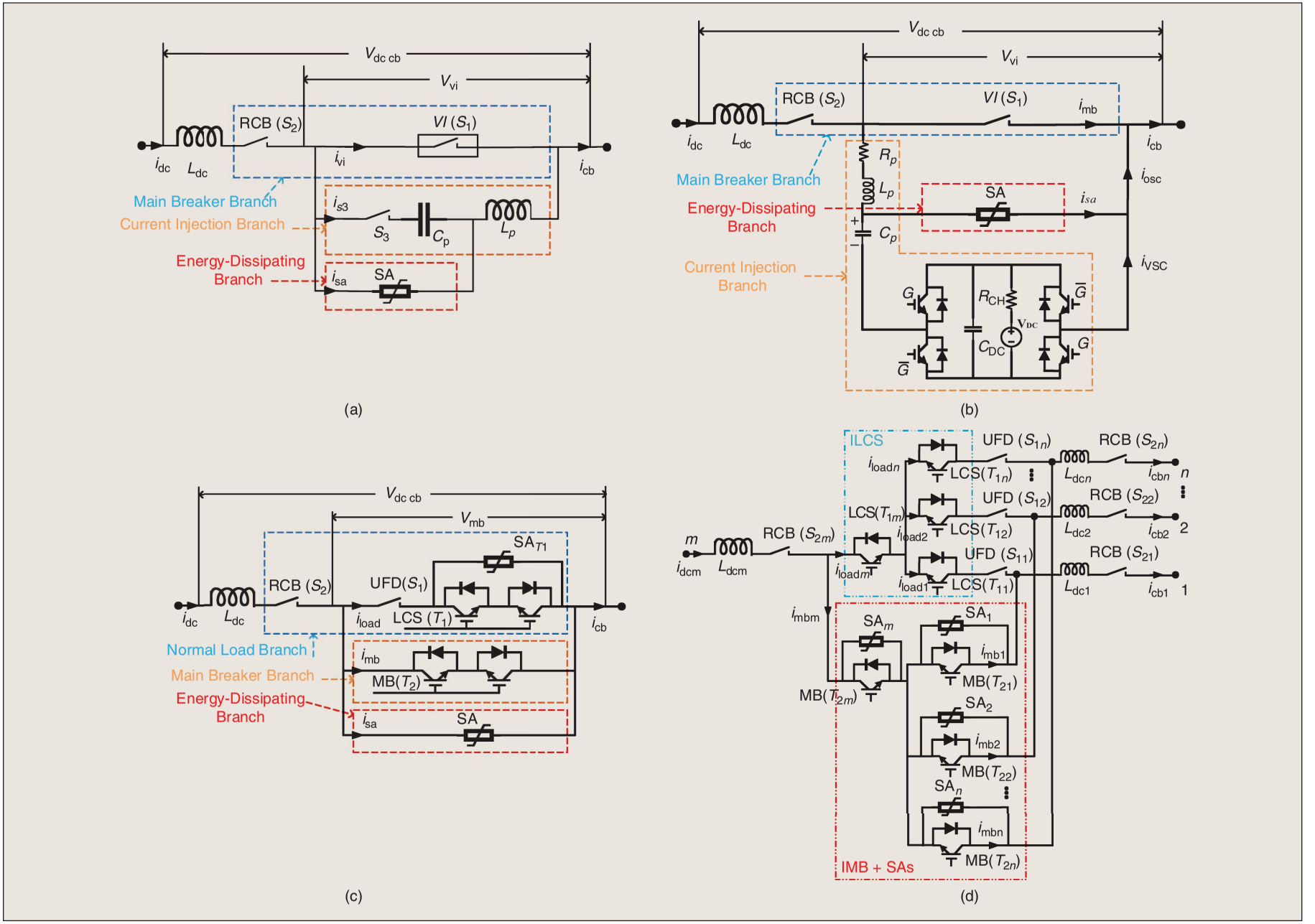

FIGURE 5 — The typical MCB, VARCCB, HCB, and multiport (MP) HCB configurations. (a) A typical MCB model, (b) a VARCCB model, (c) a classic HCB configuration, and (d) multiport HCBs. SA: surge arrester; VI: vacuum interrupter; MB: main dc breaker; IMB: integrated main breaker.

capable of passing and breaking current in reverse directions, the configuration of series- and parallel-connected IGBT modules must be capable of passing the current in both directions. Therefore, series- and parallel-connected stacks of IGBT modules are configured in antiparallel and antiseries connections. The on-state voltage drop across the IGBT modules results in permanent conduction losses in the normal load branch. As there are several IGBT modules in this branch, the conduction losses are low for HCBs. Thus, it can be seen that the performance of a typical HCB will be influenced by many factors, e.g., the snubber circuits and stray inductances in the branches, additional bidirectional current interruption capability, a cooling system for an auxiliary dc breaker and so on [51]–[54], and the breaker opening time of HCBs is in the range of 1.2–3 ms [55]. The maximum interruption current reaches 25 kA, as reported in [56].

To further decrease the capital costs and power losses of HCBs, multiport (MP) HCBs have been proposed [57], [58]. A typical MP HCB can be seen in Figure 5(d), with an integrated main breaker, an integrated load communication switch (ILCS), and more UFDs and RCBs. The general idea is to share the common branches within multiple ports connected to the same dc bus. Port m is connected to a dc bus, and ports 1–n are connected to adjacent transmission lines. However, this MP HCB is highly complex and difficult to guarantee the correct operations when the common parts are broken, e.g., the RCBs, LCSs, and MBs at the m side.

Besides classic HCBs and the related MP HCBs, several new HCB and MP HCB topologies have recently been proposed in the literature [59]–[64], only some of which are realized by low-voltage prototypes. As an example, a new HCB characterized by mixed connection of thyristors and IGBT half-bridge submodules in the main breaker is proposed in [59]. As thyristors can endure a major part of TIVs, the number of required full-controlled power semiconductors is reduced, leading to the cost reduction of HCBs. The breaking time of the proposed HCB is a bit longer than that of a fully controlled, semiconductor-based HCB. Another HCB, called a *T-type HCB*, which is based on cascaded half-bridge submodules, is introduced in [60]. A T-type HCB uses a main breaker branch composed of cascaded half-bridge submodules and diode strings instead of a conventional main breaker parallel to an LCS in a classic HCB. This topology reduces the number of required IGBTs, and it can decrease the fault peak current and breaking time.

Some other topologies have been proposed, which integrate the dc current flow control function inside MP HCBs [65], [66]. The current flow control is required in MTdc grids to prevent the lines from being overloaded. Several power electronic-based current flow controllers, such as variable resistors [67] and dc–ac and dc–dc converters, [68] and [69], respectively, are proposed for this purpose. Integrating a current flow controller inside the dc breakers reduces the costs of these solutions. An MP HCB equipped with full-bridge submodules simultaneously operating as both LCS and current flow controllers and capable of blocking the current is proposed in [65], where the submodules of the LCSs installed at adjacent lines are connected in parallel. A similar topology is presented in [66].

It should be noted that the SSCBs can be regarded as pure semiconductor switches without using any mechanical switch, which have very short breaking times but come with high costs and conduction losses [49], [70]. Therefore, it is not considered a practical solution, especially in HV levels and is not discussed in this article.

Performance Analysis for dc CB Applications in Future MTdc Grids

Time-Domain Simulation-Based Performance Comparison Among Different Types of dc CBs

In this section, four types of dc CBs are adopted for the comparison of fault current interruption:

- MCB [Figure 5(a)]
- VARCCB [Figure 5(b)]
- HCB [Figure 5(c)]
- MP HCB [Figure 5(d)]

The related parameters of these four types of dc CBs and their test systems can be found in [40], [71], and [72], respectively. The related dc voltage and interrupting current are 320 kV and 16 kA, respectively. The MP HCB is developed based on an HCB in which the parameters and the topologies of the selected HCB will be adopted and improved. The circuit for verifying the validity of the single-port dc CB models, i.e., the MCB, VARCCB, and HCB, is presented in Figure 6(a). An ideal dc source, a resistive load, and two cable branches are used in this circuit to test the target dc CB models. A revised verification circuit with one more cable branch to validate the MP dc CB model is given in Figure 6(b).

The time-domain simulations based on PSCAD/EMTDC is adopted here for the validation of system-level dc CB models [73]. The simulation results of the interruption progress can be observed in Figure 7. The signals with subscripts M, V, and H represent the related variables in MCB, VARCCB, and HCB, respectively. The fault occurs at 0.1 s, and it is located between cables 1 and 2. Then, the trip-order Kgrid from the grid protection will be received by dc CB at 0.102 s, as shown in the first row of Figure 7. The current waveforms of MCB, VARCCB, and HCB during the fault interruption can be observed from the middle rows of Figure 7, respectively. The resulting comparisons among three types of dc CBs can be easily observed by the corresponding waveforms in the same scales. The current zeros of the load branch currents (Ivi_M, Imb_V, and $Iload_H$) during the cases with MCB, VARCCB, and HCB occur at approximately 0.1101, 0.1048, and 0.103 s, before the SAs start to dissipate the energy.

From the fourth row of Figure 7, the differences of the commutation currents express the different current interruption mechanisms of MCB, VARCCB, and HCB. The comparisons of the dissipating branch currents and load

branch voltages can be observed in the third and fifth rows of Figure 7, respectively. It can be observed that the injected oscillating current in VARCCB ($Iosc_V$) reaches the zero crossing earlier than the injected current in MCB ($Is3_M$) and at almost the same instant as the main breaker current in HCB (Imb_H) is transferred from the commutation branch into the energy-dissipating branch. But with the different characteristics of SAs, the current in the HCB (Isa_H) decreases faster than the current in the VARCCB (Isa_V). Because the MP HCB is developed based on the HCB and its related parameters, nearly the same performances can be obtained. The voltages of VIs (and load branches) and the energy dissipated by those SAs are different because of the different interruption time, SA parameters, and oscillation circuits. The related differences can also been observed in Table 4, with more information from [14], [21], [32], [55], and [74].

Placement of dc CB in MTdc Grid With Considerations of dc CB Cost and FCS Selectivity

An economic comparison of solid-state CB, MCB, and two types of HCBs is given in [75], with the consideration of voltage ratings. Based on the comparative analysis in [76], the practical implementation of dc CBs will mainly consider the following factors: voltage rating, interruption time, power losses, maximum interruption current, and cost. The CIGRÉ Technique Brochure 533 reported a system-level cost analysis of HVdc systems and its related dc CB implementation, where the costs of station losses and dc CBs with different converter station topologies have been considered [21]. The cost of one 320-kV breaker is at least not more than one-sixth of a +/–320-kV converter's cost, and a 1,500-MW converter station costs roughly €150 million [21]. Also, the different choices of main components in the critical branches are considered to present the cost differences of the dc CBs at the system level, which can be observed in Table 5 [74]–[82].

For a suitable implementation at the required voltage ratings (e.g., 320 kV), one dc CB can comprise several series-connected, basic dc CB modules with lower ratings (e.g., 80 kV) [78]. For example, HCBs with ratings of 80 kV and 2 kA can be set with 3 × 3 IGBTs in LCS and 40 IGBTs in MB, considering the selected bidirectional insulated gate bipolar transistor module (4.5 kV and 3 kA) [79]. And for a 320-kV/2-kA HVdc, the HCB could comprise four cascaded 80-kV HCB modules (i.e., $3 \times 3 \times 4 + 40 \times 4$ IGBTs), or composed in the branch level (i.e., one LCS and four 80-kV MBs with $3 \times 3 + 40 \times 4$ IGBTs). The number of IGBTs will double when the bidirectional operation is considered. The MP HCB regards a more cost-efficient combination in the branch level, e.g., the one in Figure 5(b) and Table 5, is designed and is more suitable for a four-port system with the LCS, MB, and SA branches integrated and shared between every two ports. Even though there are different dc CB solutions, when HV electrical systems and their related protection systems are considered with the selectivity of the FCS, the placement of a dc CB system can be further investigated [24], which can be conducted by the workflow shown in Figure 8.

A symmetric-monopole, three-terminal HVdc grid with half-bridge MMCs, as depicted in Figure 2, is chosen for study here, in which the half-bridge MMC is without fault interruption functions and one dc CB is assumed to be installed at the converter terminal. Then, the required number of dc CBs for different FCSs are provided in Table 6. Here, for each option of the FCS, only the application cases with typical dc CBs are chosen for a general comparison; thus, the ac CB-based nonselective FCS will not be contemplated here. For partially selective FCSs, a triangle HVdc transmission topology can, at least, be divided into two subgrids with two more dc CBs (e.g., the case in Figure 8), and at most, five zones with five more dc CBs (when one line and one bus are covered by one zone). It can be seen from Table 6 that the selectivity of the FCS will be largely determined by the dc CB's number and placement, and the cheapest FCS is the nonselective one with the least placement of dc CBs and the lowest selectivity.

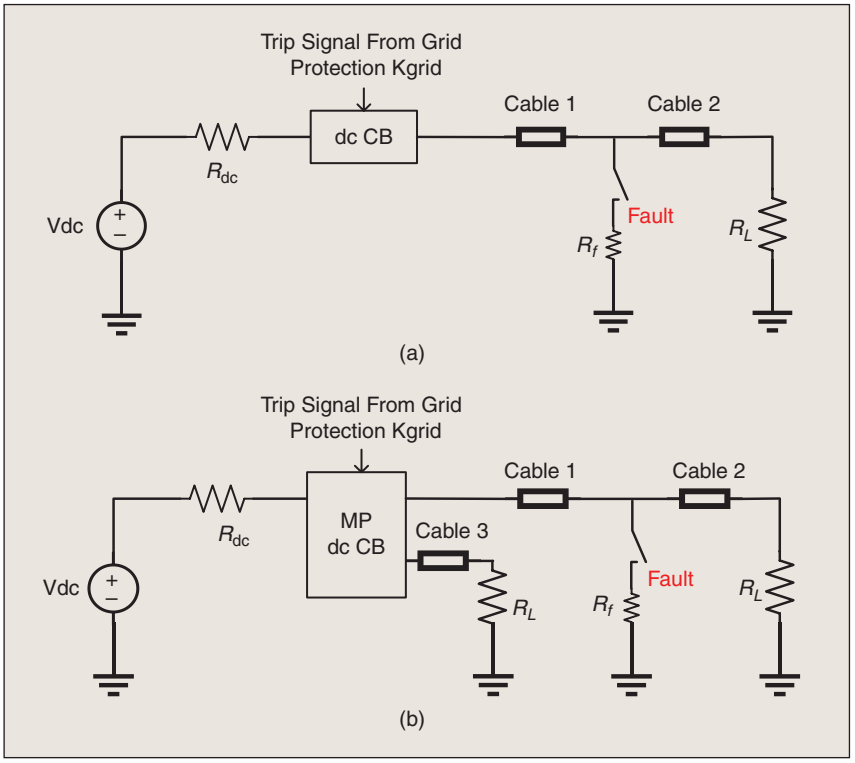

FIGURE 6 — The verification circuits for used testing typical dc CB models. (a) A simple verification circuit for single-port dc CBs. (b) The revised verification circuit for MP dc CBs.

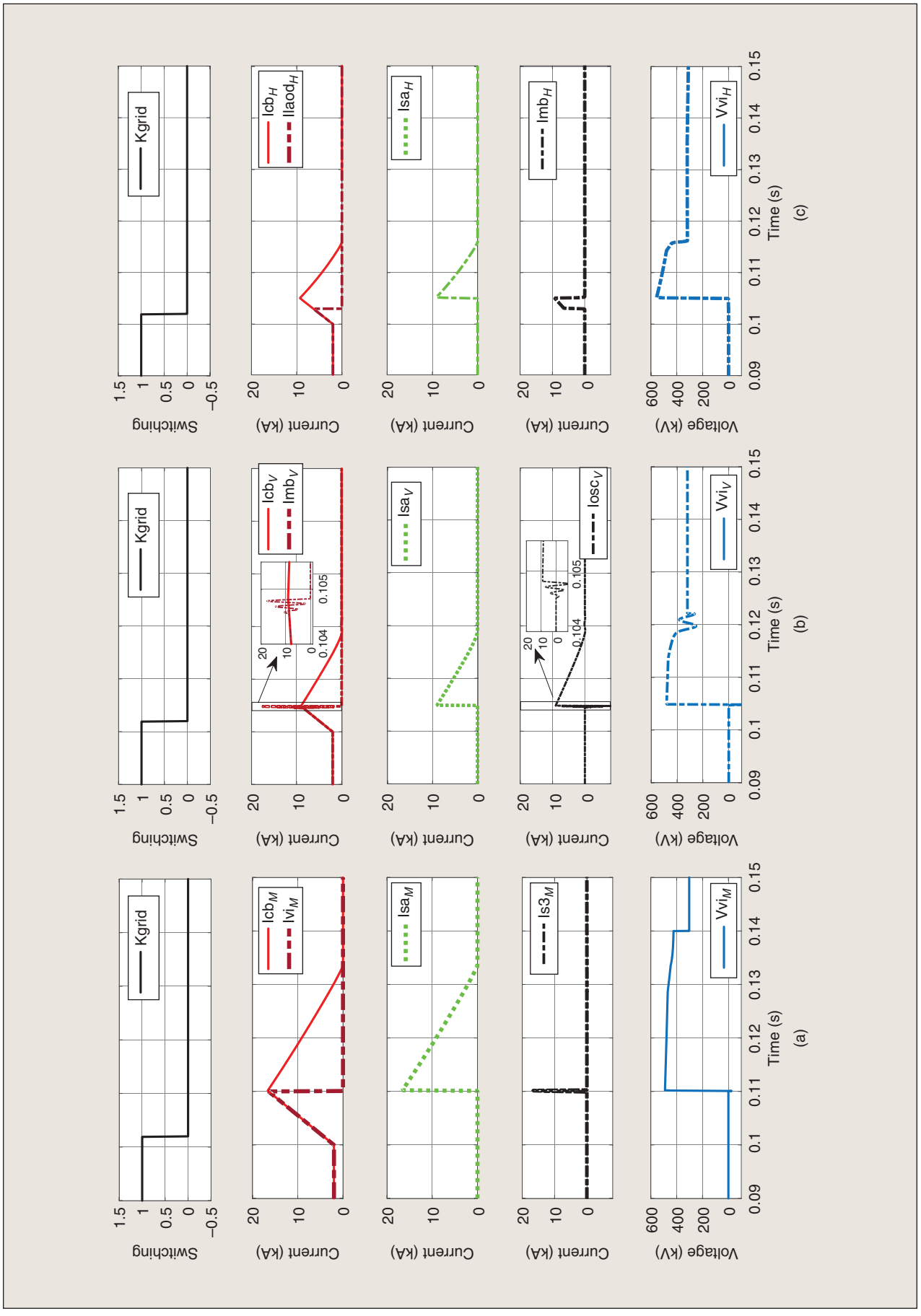

FIGURE 7 – The simulation results of typical dc CB models in the test circuits. The interruption waveforms of (a) MCB, (b) VARCCB, and (c) HCB.

TABLE 4 — A COMPARISON OF THE DIFFERENT TYPES OF dc CBs.

	CLASSIC HCB	MP HCB	VARCCB	MCB
Nominal current branch	UFD- and IGBT-based LCSs	UFD- and IGBT-based LCSs	VI	VI
Commutation branch	IGBT-based main breaker	IGBT-based main breaker	VSC- and LC-based injection circuits	LC-based injection circuit
Interruption mechanism	The current flowing through the nominal current branches is transferred into the main breaker branch to interrupt.	The current flowing through the nominal current branches is transferred into the main breaker branches to interrupt.	The VSC injects the oscillation current with increasing amplitude in every half cycle to create a zero in the nominal current branch for vacuum interruption.	The precharged injection circuit injects the current for creating a current zero in the nominal current branch for vacuum interruption.
Maximum interruption current (kA)	16–25	16–25	9–16	16
Breaking time (ms)	2–5	2–5	2–8	5–10
On-state losses	High	High	Low	Low
Development state	320-kV prototype; 500 kV is under development	Under research for 320 kV	27- and 80-kV prototypes; 320 kV is under research	160 kV is in operation
TIV (p.u.)	1.6	1.6	1.51	1.53
Dissipated energy (MJ)	Low	Low	Low	High

p.u.: per unit.

Apart from the selectivity, which depends on the number of protection zones and dc CBs, the cost and speed cannot be easily defined. When a fully selective FCS is required with the implementation of 18 dc CBs, the solution with MCBs are much cheaper than the one with HCBs, and the lower speed of the MCBs could be accepted. However, with newly developed VARCCBs, a lower-cost increment than HCBs can obtain higher speeds than the MCB solution. Moreover, if the fully selective FCS is pondered with MP HCB implementation, the cost will be largely decreased from the classic HCB solution, and the speed performance will be better than that of the MCB and VARCCB solutions. Thus, from the perspectives of cost and speed, the VARCCB and MP HCB solutions will be better than the other solutions.

Considering that there is still a large cost difference between the VARCCB and MP HCB solutions, more cost considerations on the requirements of on-state losses, system-stability constraints, dc CB-related parameter optimization, and control system complexity need to be further investigated [21], [75]. Also, the cost- and speed-related performances and criteria of dc CBs would change because of market situations and technology innovations, and the different dc CBs would be exposed to different risks, e.g., the possible failure of common switches in MP HCBs and the diverse difficulties during repeated fault interruption and reclosing [49], [82]. When system-wide coordinative protection and control are considered, the different issues among converter control, fault current limiters, and ac CB-/dc CB-based protective control during fault clearing and system recovery will be complicated and significant [24]. Thus, for future investigation, besides the selectivity, cost, and speed, more factors related to the reliability and robustness of those new solutions (such as in [65] and [66]) on a system-wide level could be of importance [52], which can help find the most suitable solution for the security of future MTdc grids.

Coordination and Testing Investigation of dc CBs in Future MTdc Grids

Reclosing and Recovering Function

To ensure power system security and stability, MTdc grids must be able to quickly recover power transmission after fault clearing. Subsequent to the isolation of overhead lines in case of a transient fault, dc CBs must perform reclosing to recover power transmission. In a conventional reclosing strategy, dc CBs will automatically reclose

TABLE 5 — THE APPROXIMATE COST COMPARISON OF DIFFERENT TYPES OF dc CBs.

		CLASSIC HCB [76]–[78]	MP HCB [81]	VARCCB [49], [50], [80]	MCB [75], [80]
Voltage rating (kV)		320	320	320	320
Topology consideration	**Nominal current branch**	3 × 3 IGBTs in LCSs	In Figure 5(b), 3 × 3 × 4 IGBTs in the ILCSs	VI	VI
	Commutation branch	160 IGBTs in the MB	160 × 4 IGBTs in the IMB	IGBT (3 × 4 × 4)-based VSC injection circuit	LC-based injection circuit
	Energy-dissipating branch	Metal oxide SA	Metal oxide SA × 4	Metal oxide SA	Metal oxide SA
Cost		Very high	High	Medium	Low

IMB: integrated main breaker.

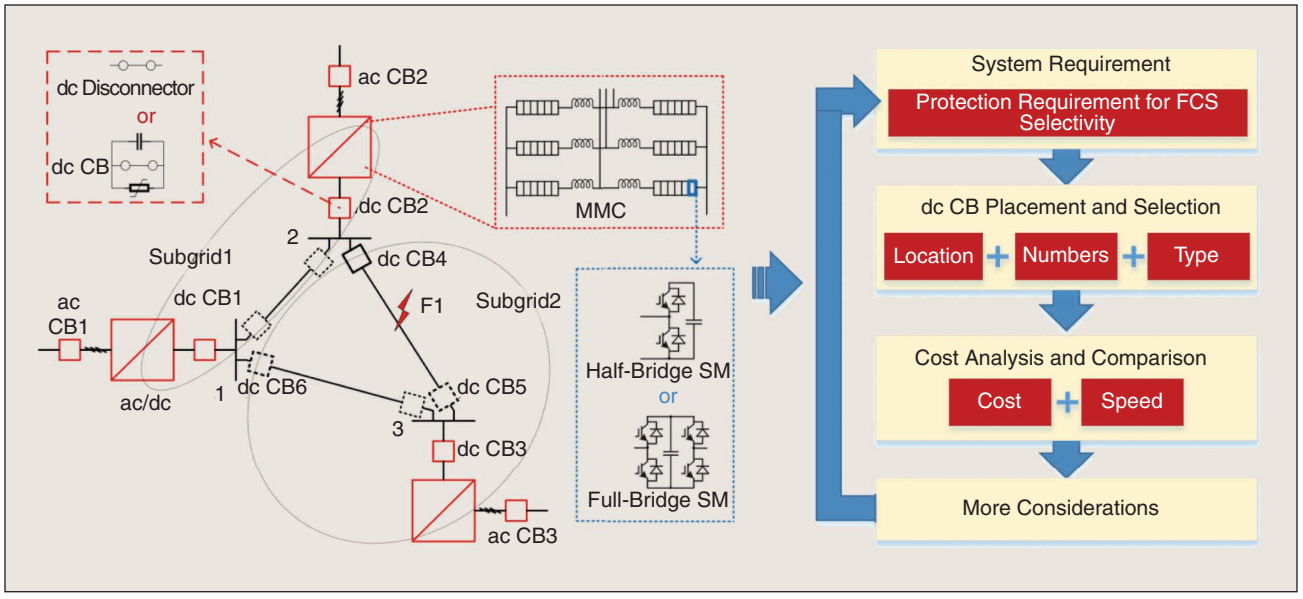

FIGURE 8 — The workflow of a cost-based dc CB planning considering the FCSs in an MTdc grid.

within a predefined time to ensure the arc deionization of a faulted overhead line. The time sequence of conventional reclosing is shown in Figure 9. However, reclosing under permanent fault will deteriorate the overcurrent issues in MTdc grids, which raises a high requirement of the dc CB interruption capacity [83]. To prevent a reclosing under permanent fault, adaptive reclosing schemes have been proposed to determine suitable reclosing operations for different fault types, i.e., permanent or transient. An adaptive reclosing scheme with HCBs, using active voltage pulse injection from the associated converter, is proposed in [84]. A similar method based on active pulse injection using hybrid MMCs, including both half- and full-bridge submodules in the arms, is proposed in [85]. Two fault-type identification methods based on the measuring line residual voltage are proposed in [86] and [87]. In these methods, only the RCB is required to be reclosed for fault-type identification, and therefore, they can be applied in case of MCBs and VARCCBs.

To avoid potential adverse impacts such as maloperation of the protection system, line insulation failure, and to reduce stresses on power electronic devices resulting from reclosing dc CBs in one stage, sequential or soft reclosing schemes have been offered in [88] and [89]. These schemes make use of controllable cascaded submodules in the commutation branch of HCBs. And the rate of rise

TABLE 6 — THE REQUIRED NUMBER OF dc CBs FOR DIFFERENT FCSs.

	OPTIONS OF FCSs	dc CB PLACEMENT		NUMBER OF dc CBs (N)
1	Fully selective FCSs	Six protection zones	At each end of the dc branches and buses	18
2	Partially selective FCSs	Five protection zones	At the borders of the protection zones, and the number of zones will decrease when one zone covers more branches and buses, e.g., two zones are composed in Figure 8, only dc CB4, dc CB6, and dc CB3 are installed in subgrid2, and only dc CB1 and dc CB2 are installed in subgrid1.	16
		Four zones		14
		Three zones		12
		Two zones		10
3	Nonselective FCSs	One zone in the grid	Only the dc CBs at the converter sides are installed, e.g., dc CB1, dc CB2, and dc CB3.	6

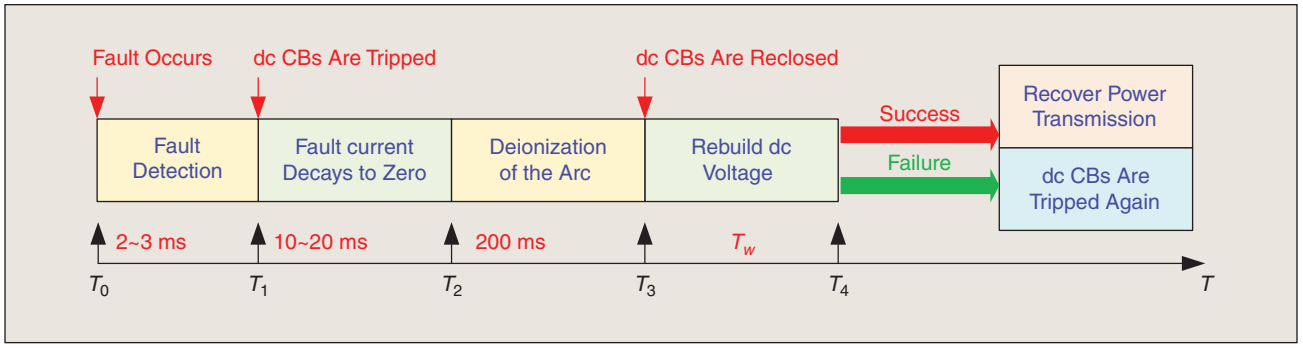

FIGURE 9 — The time sequence of a conventional reclosing [84].

of voltage and current are limited by the step-by-step operation of the submodules in the commutation branch of HCBs. The dc voltage at the line side of HCBs is checked to determine if the fault is eliminated or if it is permanent. The schemes can be implemented at both ends of the line and can eliminate the need for communication links between the line ends used for reclosing. Moreover, multiple autoreclosing operations can be conducted as the dissipated energy is negligible here.

Testing Requirements and Considerations

Currently, there are no standards on the test requirements and procedures of dc CBs. The simultaneous presence of the voltage and current of dc CBs during current interruption results in energy absorption requirements and therefore, the testing of dc CBs is fundamentally different than that of ac CBs. A meaningful validation of dc CBs can be made when the tests accurately reflect the practical conditions occurring in real HVdc systems. The generic test requirements can be categorized into four types, i.e., dielectric, operational, breaking, and endurance tests [30], [31]. The short circuit current breaking test is the most important and challenging one because there is a high requirement of a sufficient capability for supplying high rising rates of fault current.

For a basic concept and topology validation, an offline electromagnetic transient simulation is normally used, which may have an impractical simulation time and simplified models [90]. A multiphysics simulation can also be adopted when the plasma and thermal effects have been considered in dc CB modeling [47], [91]. As HVdc CBs are very expensive and interact strongly with the related dc protection and MTdc grids, power-hardware-in-the-loop (PHIL) methods become popular to test the system-level cooperation performances of dc CBs and protection, where complex HVdc system operation conditions can be simulated, and the dc CB prototypes are normally built in a low power level [12], [92]. In PHIL testing methods, a suitable power amplifier will be applied to generate the required short circuit voltage and current for testing dc CB prototypes, which is not needed during the offline simulation and validation stages.

The full-power testing of dc CB prototypes could be conducted in synthetic testing [93]. Due to a lack of HVdc synthetic test circuit design experiences, the standard of an ac synthetic test is normally adopted as the reference of a dc synthetic test method design. Several synthetic dc CB test circuits are investigated in [40], [94], and [95]. A synthetic test circuit composed of ac short circuit generators operating at low frequency is proposed by KEMA [96], as shown in Figure 10. The test circuit provides all of the generic requirements, and it can be used for the full-power testing of dc CBs, especially when the breaking process is much shorter than the half cycle of a generator's voltage. Moreover, the ac short circuit generators are already available because they are being used for ac equipment testing.

As depicted in Figure 10, the test circuit comprises four parts, the power source, overcurrent protection, a dc voltage source for dielectric stress, and an arcing time-prolongation circuit part. The power source part, which is formed from low-frequency, ac short circuit generators and power transformers, supplies the required current, voltage, and energy during the current interruption. The overcurrent protection part, including a plasma-triggered spark gap (that is, TSG1) and an auxiliary high-voltage ac time-prolongation part provides

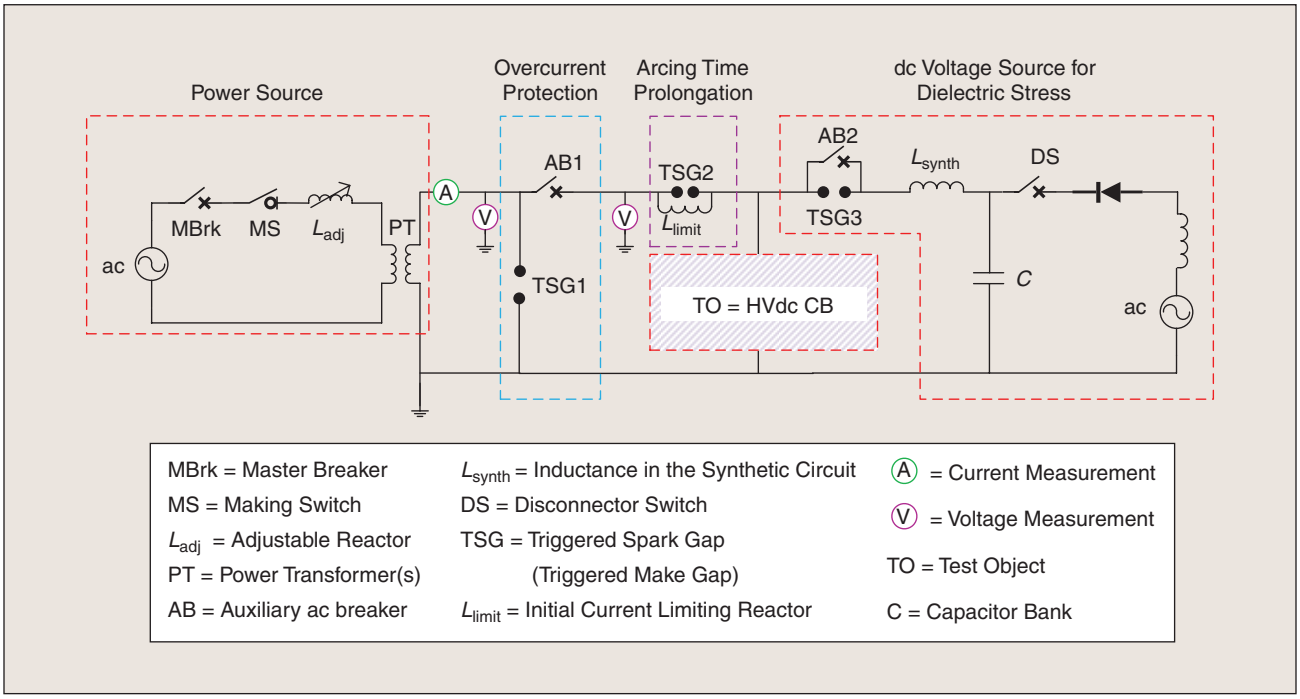

FIGURE 10 — The circuit used for testing the dc CB's performance [96].

an additional arcing time for AB1 to build the required test current with a specific rate of rise. According to the aforementioned discussions and considerations, the related comparisons among the different simulation and testing methods on the validation stages, focuses, requirements, and capabilities can be observed in Table 7.

Remaining Challenges and Future Needs

According to the presented details concerning the dc CB applications in HVdc power systems, several main technological areas have been investigated and discussed, where further R&D is still required to improve the dc CB capabilities to deal with the remaining challenges. The four main areas are summarized as follows.

The Breaker Architecture and Multiphysic Simulation

To make a reliable configuration of a dc CB, its architecture must be accounted for as the dc CB normally consists of electrical, mechanical, and thermal components. The operation of such a complex system results in different physical phenomena. Therefore, the comprehensive analysis and design of a dc CB requires a multiphysical and/or finite element-based models that can predict the different phenomena and characteristics with a required degree of accuracy to investigate the effects related to the mechanical structure, acoustics, electromagnetic coupling, and heat transfer. As a result, the architecture of a dc CB can be optimized.

Coordination With Protection, Control, and FCSs

It can be seen from previous discussions that dc fault characteristics are defined by ac and dc system parameters and their related fault current control strategies [97], which are challenging for the design and testing of dc CBs. Especially for the reliability of the whole MTdc grid, the reclosing and recovering functions are also required as parts of the dc system protection strategies. All of these considerations and requirements express the significance of the coordination between the dc CB and the protection and control strategies during the planning, design, and operation stages of dc CBs and protection systems. In addition, as the interactions between converter fault controls and dc reactor designs depend on different converter topologies and ratings, the system-level coordination between dc CB-based protection systems, MMC-based control systems, and MTdc grid configurations are important to realize effective fault clearing and post-fault recovery. The global optimization of the whole system, including dc CBs, control, and protection, is expected in the future design and operation of MTdc grids.

Synthetic Evaluation System for dc CB Modeling and Reliable Operation

Due to the increasing complexity of dc CB modeling and its related system-level interactions, its performance evaluation must be redefined according to the dimensions of the dc CB's multiphysic models. Moreover, various kinds of failure modes in different levels can be developed for both internal and external interactions of dc CBs, e.g., the interruption failure of VIs in MCBs or the coordination failure between dc CBs and converter fault control. Thus, such a challenge necessitates identifying the possible failure models of existing dc CB technologies in the related synthetic evaluation system for a reliable fault clearing in future HVdc grids.

Testing and Standardization

In addition to the synthetic testing of full-pole dc CBs, the multilayer test system can be used in a way to test the HV dc CB component by component, branch by branch, unit by unit, and then it can be upgraded for an HVdc system-level application testing. Reliability testing on common branches, especially in the case of MP HCBs, will define the final quality and feasibility of dc CBs. In this way, the mechanism and concepts for both the component and system levels can be thoroughly validated by applying the appropriate evaluation systems, which can provide sufficient information to perform dc CB design optimization, standardization, and industrial production. Considering that different dc CBs and HVdc solutions from more than one manufacturer may exist in the new

TABLE 7 — COMPARISONS OF THE DIFFERENT SIMULATION AND TESTING METHODS.

	OFFLINE SIMULATION	MULTIPHYSICS SIMULATION	PHIL TESTING	FULL-POWER TESTING
Validation stage	Basic concept and topology level	Detailed component level	Prototyping and partly the prototyping level	Final product level
Validation focus	• Electromagnetic transient simulation	• Electromagnetic transient • Arc plasma • Thermal progress	• Complex simulation scenarios • Cooperative operation test • Related operation limits	• A synthetic test, including all of the focuses • Security, reliability, compatibility, and so on
Requirements	• Simulated testing conditions • Concept-/component-level dc CB models	• Simulated testing conditions • Specific component-level dc CB models	• Simulated testing conditions • Specific component-level dc CB models • Low-power prototype or a part of the prototype • Effective power amplifier to generate the short circuit current	• A synthetic test circuit composed of ac short circuit generators to provide short circuit current • Related protection for the test circuit • dc voltage source for testing dielectric stress • Arcing time-prolongation circuit • Full-pole dc CB prototype
Capability	Current-breaking test	Dielectric, breaking, and endurance tests	Dielectric, operational, breaking, and endurance tests	Dielectric, operational, breaking, and endurance tests

MTdc grids, the interoperability issues cannot be ignored as well. The standardizations for the MTdc grids and their related protection systems are particularly significant, especially for dc CBs and their coordination with the power network and protection systems.

Conclusion

In this article, an overview of the developments and challenges of HVdc CB technologies was presented, which pave the way for future applications. As an important component to secure the operation of MTdc grids, dc CBs have been under R&D since the 1940s for different generations of HVdc systems. Compared to ac CBs, the operations and requirements of dc CBs are different due to the complexity of modern hybrid ac–dc power systems and their related control strategies. The classical types of dc CBs have been investigated and compared, based on a literature overview, time-domain simulation, and cost analysis. By taking into account protection strategies with different selectivity requirements, the optimal solutions of dc CBs can be defined according to cost-optimization functions. The reclosing and recovering functions of dc CBs were also discussed in this article, and they deserve more attention with respect to the protection and control operation of future MTdc grids. Moreover, more intelligent and comprehensive evaluation and testing systems are required for dc CBs as they will be the basis for future standardization related to MTdc grid operation.

Acknowledgments

The corresponding author is Zhou Liu.

Biographies

Zhou Liu (zli@et.aau.dk) earned his Ph.D. degree in energy technology from Aalborg University (AAU), Denmark, in 2013. Since December 2014, he has worked as a postdoctoral researcher at the Department of Electric Power Engineering, the Norwegian University of Science and Technology. He is currently an assistant professor in the Department of Energy Technology, AAU, Aalborg, 9220, Denmark. From 2017 to 2018, he worked as a postdoctoral fellow at the Department of Electrical Sustainable Energy, TU Delft, The Netherlands. He has been involved in the Progress on Meshed HVdc Offshore Transmission Networks project at TU Delft. He is a Senior Member of IEEE.

Seyed Sattar Mirhosseini (s_mirhoseini@elec.iust.ac.ir) earned his Ph.D. degree in electrical engineering from the Iran University of Science and Technology, Tehran, Iran, in 2021. His research interests include power system protection, in particular, the protection of multiterminal high-voltage dc (HVdc) grids and HVdc circuit breakers. He has been involved in the Progress on Meshed HVdc Offshore Transmission Networks project as a visiting researcher at TU Delft, The Netherlands. He is a Student Member of IEEE.

Lian Liu (lian.liu@prysmiangroup.com) earned his Ph.D. degree from the Department of Electrical Sustainable Energy, Delft University of Technology (TU Delft), Delft, The Netherlands, in 2019. His research interests include power system modelling and protection, especially, the protection of multiterminal high-voltage dc (HVdc) grids. His Ph.D. program was financed by the China Scholarship Council. From 2017 to 2018, he was a research associate with the Department of Electrical Sustainable Energy, Tu Delft in the project Electric "Transmission and Storage Options" for 2020. He has been involved in the Progress on Meshed HVdc Offshore Transmission Networks project at TU Delft.

Marjan Popov (M.Popov@tudelft.nl) earned his Ph.D. degree in electrical power engineering from Delft University of Technology, Delft, The Netherlands, in 2002. He is a member of CIGRE and actively participated in Working Group (WG) C4.502 and WG A2/C4.39. He was a recipient of the IEEE PES Prize Paper Award and the IEEE Switchgear Committee Award in 2011. He is an associate editor of *International Journal of Electric Power and Energy Systems*. In 2017, he founded the Dutch Power System Protection Centre to promote research and education in intelligent power system protection. He is a Senior Member of IEEE.

Kaiqi Ma (kma@et.aau.dk) earned his M.Sc. degree from Hohai University, Nanjing, China, in control engineering in 2015. He was a research associate at the Research & Development Center of State Grid Xuji Group Corporation, China. Since 2018, he has been a Ph.D. student at the Department of Energy Technology, Aalborg University, Denmark. His research interests include distributed generation, wind power generation, and relay protection. He is a Student Member of IEEE.

Weihao Hu (whu@uestc.edu.cn) is a full professor and director of the Institute of Smart Power and Energy Systems at the University of Electronics Science and Technology of China, 611731, China. He has led/participated in more than 15 research projects and has more than 140 publications. He has been a guest editor of the *IEEE Transactions on Power Systems* Special Section: Enabling Very High Penetration Renewable Energy Integration Into Future Power Systems. He served as the technical program chair for IEEE Innovative Smart Grid Technologies Asia 2019. He is a Senior Member of IEEE and a member of the IEEE Industrial Electronics Society.

Sadegh Jamali (sjamali@iust.ac.ir) earned his Ph.D. degree in electrical engineering from the University of London, London, U.K., in 1990. He is currently with the School of Electrical Engineering at Iran University of Science and Technology, Tehran, 13114-16846, Iran. His research interests include power system protection, distribution systems, and railway electrification, where he is heavily involved in industrial consultancy. He is a fellow of the Institution of Engineering and Technology, and a chartered engineer in the United Kingdom.

Peter Palensky (P.Palensky@tudelft.nl) is a professor of intelligent electric power grids at Delft University of Technology (TU Delft), Delft, 2600 AA, The Netherlands. Previously, he was a principal scientist for Complex Energy Systems at the Austrian

Institute of Technology (AIT), Energy Department, Austria; head of Business Unit Sustainable Building Technologies at the AIT; and an associate professor at the University of Pretoria, South Africa. He works on the digital aspects of intelligent energy systems and operates a real-time digital simulator-based power system digital twin at TU Delft. He is a Senior Member of IEEE and a member of the IEEE Industrial Electronics Society.

Zhe Chen (zch@et.aau.dk) earned his Ph.D. degree in electrical engineering from the University of Durham, Durham, U.K. He is a full professor with the Department of Energy Technology, Aalborg University (AAU), Aalborg, 9220, Denmark. He is the leader of the Wind Power System Research Program with the Department of Energy Technology, AAU, and the Danish Principle Investigator for Wind Energy of Sino-Danish Centre for Education and Research. He is a Fellow of IEEE and of the Institution of Engineering and Technology, a chartered engineer in the United Kingdom, and a member of the IEEE Industrial Electronics Society.

References

[1] H. Li and Z. Chen, "Overview of different wind generator systems and their comparisons," *IET Renew. Power Generation*, vol. 2, no. 2, pp. 123–138, 2008. doi: 10.1049/iet-rpg:20070044.

[2] "Québec – New England, the first large scale multiterminal HVDC transmission in the world to be upgraded," ABB, Västerås, Sweden, 2016. [Online]. Available: https://new.abb.com/systems/hvdc/references/quebec-new-england

[3] G. Bathurst and P. Bordignan, "Delivery of the Nan'ao multi-terminal VSC-HVDC system," in *Proc. 11th IET Int. Conf. AC and DC Power Transmiss.*, 2015, pp. 1–6. doi: 10.1049/cp.2015.0029.

[4] G. Tang, Z. He, H. Pang, X. Huang, and X. Zhang, "Basic topology and key devices of the five-terminal DC grid," *CSEE J. Power Energy Syst.*, vol. 1, no. 2, pp. 22–35, 2015. doi: 10.17775/CSEEJPES.2015.00016.

[5] G. Li, J. Liang, S. Balasubramaniam, T. Joseph, C. E. Ugalde-Loo, and K. F. Jose, "Frontiers of DC circuit breakers in HVDC and MVDC systems," in *Proc. IEEE Conf. Energy Internet Energy Syst. Integr.*, 2017, pp. 1–6.

[6] A. Greenwood, K. Kanngiessner, V. Lesclae, T. Margaard, and W. Schultz, "Circuit breakers for meshed multiterminal HVDC systems. Part I: Introduction DC side substation switching under normal and fault conditions," *Electra*, vol. 163, no. 4, pp. 98–122, 1995.

[7] S. Liu and M. Popov, "Development of HVDC system-level mechanical circuit breaker model," *Int. J. Electr. Power Energ. Syst.*, vol. 103, pp. 159–167, Dec. 2018. doi: 10.1016/j.ijepes.2018.05.017.

[8] X. Pei, O. Cwikowski, D. S. Vilchis-Rodriguez, M. Barnes, A. C. Smith, and R. Shuttleworth, "A review of technologies for MVDC circuit breakers," in *Proc. 42nd Annu. Conf. IEEE Ind. Electron. Soc. (IECON 2016)*, Florence, Italy, 2016, pp. 3799–3805. doi: 10.1109/IECON.2016.7793492.

[9] Z. Zhang et al., "Research and development of an ultra-fast 160kV mechanical HVDC circuit breaker," *Power System Technol.*, vol. 42, no. 7, pp. 2331–2338, 2018.

[10] "Thomas Edison," Wikipedia, 2019. [Online]. Available: https://en.wikipedia.org/wiki/Thomas_Edison

[11] P. Brückner, "Abschalten einer in Betrieb befindlichen Gleichstromleistung," Germany Patent B 207 592, Nov. 20, 1944.

[12] C. M. Franck, "HVDC circuit breakers: A review identifying future research needs," *IEEE Trans. Power Del.*, vol. 26, no. 2, pp. 998–1007, 2011. doi: 10.1109/TPWRD.2010.2095889.

[13] S. Tokuyama, K. Arimatsu, Y. Yoshioka, and Y. Kato, "Development and interrupting tests on 250 KV 8 KA HVDC circuit breaker," *IEEE Trans. Power App. Syst. * (through 1985)*, vol. PAS-104, no. 9, pp. 2452–2459, 1985. doi: 10.1109/TPAS.1985.318990.

[14] B. Pauli, G. Mauthe, E. Ruoss, and, G. Ecklin, "Development of a high current HVDC circuit breaker with fast fault clearing capability," *IEEE Trans. Power Del.*, vol. 3, no. 4, 1988, pp. 2072–2080. doi: 10.1109/61.194019.

[15] G. Asplund, K. Svensson, H. Jiang, J. Lindberg, and R. Pålsson, "DC transmission based on voltage source converters," in *Proc. CIGRÉ Session*, Paris, France, 1998, pp. 1–8.

[16] A. Lesnicar and R. Marquardt, "An innovative modular multilevel converter topology suitable for a wide power range," *Proc. IEEE Power Tech Conf.*, Bologna, 2003, pp. 1–6.

[17] J. Häfner and B. Jacobson, "Proactive hybrid HVDC breakers—A key innovation for reliable HVDC grids," *Proc. CIGRÉ Bologna Symp.*, Bologna, 2011, pp. 1–9.

[18] Z. Jie et al., "Research of DC circuit breaker applied on Zhoushan multi-terminal VSC-HVDC project," in *Proc. IEEE PES Asia-Pacific Power Energy Eng. Conf. (APPEEC)*, 2016, pp. 1636–1640.

[19] "Mitsubishi electric achieves successful fault current interruption using 160kV DC circuit breaker," Mitsubishi Electric, Tokyo, Japan, 2019. Available: https://emea.mitsubishielectric.com/en/news/releases/global/2019/1010-a/index.html

[20] "SCiBreak 80 kV modular HVDC breaker successfully tested at KEMA," CiBreak AB, JÄRFÄLLA, Sweden. Accessed: Aug. 20, 2020. Available: https://www.scibreak.com/?p=95121

[21] "HVDC grid feasibility study," CIGRÉ Working Group B4.52, TB-533, 2013. [Online]. Available: https://e-cigre.org/publication/533-hvdc-grid-feasibility-study

[22] R. Li, L. Yu, L. Xu, and G. P. Adam, "DC fault protection of diode rectifier unit based HVDC system connecting offshore wind farms," *IEEE Power Energ. Soc. General Meeting (PESGM)*, 2018, pp. 1–5.

[23] O. E. Oni, I. E. Davidson, and K. N. I. Mbangula, "A review of LCC-HVDC and VSC-HVDC technologies and applications," in *Proc. IEEE 16th Int. Conf. Environ. Electr. Eng.*, Florence, Italy, 2016.

[24] "Protection and local control of DC grids," CIGRÉ Working Group B4/B5-59, CIGRÉ TB-739, 2018.

[25] Z. Liu et al., "Protection testing for multiterminal high-voltage dc grid: Procedures and procedures and assessment," *IEEE Ind. Electron. Mag.*, 2020. vol. 14, no. 3, pp. 46–64, doi: 10.1109/MIE.2020.2977150.

[26] R. Dantas, J. Liang, C. E. Ugalde-Loo, A. Adamczyk, C. Barker, and R. Whitehouse "Progressive fault isolation and grid restoration strategy for MTDC networks," *IEEE Trans. Power Del.*, vol. 33, no. 2, pp. 909–918, 2018. doi: 10.1109/TPWRD.2017.2720844.

[27] S. Wenig, M. Goertz, C. Hirsching, M. Suriyah, et al. "On full-bridge bipolar MMC-HVDC control and protection for transient fault and interaction studies," *IEEE Trans. Power Del.*, 2018. vol. 33, no. 6, pp. 2864–2873, doi: 10.1109/TPWRD.2018.2823770.

[28] N.Johannesson, S. Norrga, and M. C. Wikstro, "Selective wave-front based protection algorithm for MTDC systems," in *Proc. 13th Int. Conf. Dev. in Power Syst. Protection (DPSP)*, Stevenage, 2016. doi: 10.1049/cp.2016.0051.

[29] L. Zhang et al., "Modeling, control, and protection of modular multilevel converter-based multi-terminal HVDC systems: A review," *CSEE J. Power Energy Syst.*, vol. 3, no. 4, pp. 340–352, 2017. doi: 10.17775/CSEEJPES.2017.00440.

[30] N. A. Belda, C. A. Plet, and R. P. P. Smeets, "Analysis of faults in multiterminal HVDC grid for definition of test requirements of HVDC circuit breakers," *IEEE Trans. Power Del.*, vol. 33, no. 1, pp. 403–411, 2018. doi: 10.1109/TPWRD.2017.2716369.

[31] N. A. Belda, C. A. Plet, R. P. P. Smeets, and R. Nijman, "Stress analysis of HVDC circuit breakers for defining test requirements and its implementation," in *Proc. CIGRE Colloq.*, 2017. pp. 1–11.

[32] "Technical requirements and specifications of state-of-the-art DC switching equipment," CIGRÉ Joint Working Group A3-B4.34, CIGRÉ TB-683, 2017. [Online]. Available: https://e-cigre.org/publication/683-technical-requirements-and-specifications-of-state-of-the-art-hvdc-switching-equipment

[33] B. Li, F. Jing, B. Li, W. Wen, and "Research on the parameter matching between active SI-SFCL and DC circuit breaker in DC systems," *IEEE Trans. Appl. Supercond.*, vol. 29, no. 2, pp. 1–5, 2019. doi: 10.1109/TASC.2019.2892519.

[34] "System aspects of HVDC grids," CENELEC, Brussels, Belgium, CENELEC TC 8X/WG 06, 2016. [Online]. Available: https://www.cenelec.eu

[35] *IEEE Standard for AC High-Voltage Circuit Breakers Rated on a Symmetrical Current Basis- Preferred Ratings and Related Required Capabilities for Voltages Above 1000 V*, IEEE Standard C37.06, 2009.

[36] L. Storasta, M. Rahimo, J. Haefner, F. Dugal, E. Tsyplakov, and M. Callavik, "Optimized power semiconductors for the power electronics based HVDC breaker application," in *Proc. PCIM Europe 2015*, 2015, pp. 1–6.

[37] P. Skarby and U.Steiger, "An ultra-fast disconnecting switch for a hybrid HVDC breaker—A technical breakthrough," in *Proc. CIGRÉ Session*, Alberta, Canada, Sept. 2013, pp. 1–9.

[38] K. Tahata et al., "HVDC circuit breakers for HVDC grid applications," in *Proc. AORC-CIGRÉ*, Tokyo, 2015, pp. 1–9.

[39] U. Margi and S. Priyank, "A review on HVDC circuit breakers," *Int. J. Eng. Comput. Sci.*, vol. 5, no. 6, pp. 17,110–17,115, 2016.

[40] M. Callavik, A. Blomberg, J. Hafner, and B. Jacobson, "The hybrid HVDC breaker: An innovation breakthrough enabling reliable HVDC grids," ABB Grid Syst., Zurich, Tech. Paper, Nov. 2012, pp. 1–10.

[41] R. Yeckley and J. Perulfi, "Oil circuit breakers: A look at the earlier generation [history]," *IEEE Power Energy Mag.*, vol. 16, no. 3, pp. 86–97, 2018, doi: 10.1109/MPE.2018.2801959.

[42] B. Bachmann, G. Mauthe, E. Ruoss, H. Lips, and J. Vithayathil, "Development of a 500 kV airblast HVDC circuit breaker," *IEEE Trans. Power App. Syst. * (through 1985)*, 1985. vol. PAS-104, no. 9, pp. 2460–2466, doi: 10.1109/TPAS.1985.318991.

[43] J. Fontchastagner, O. Chadebec, H. Schellekens, G. Meunier, V. Mazauric, "Coupling of an electrical arc model with FEM for vacuum interrupter designs," *IEEE Trans. Magn.*, 2005. vol. 41, no. 5, pp. 1600–1603, doi: 10.1109/TMAG.2005.845023.

[44] H. Nakao et al., "DC current interruption in HVDC SF6 gas MRTB by means of self-excited oscillation superimposition," *IEEE Trans. Power Del.*, 2001. vol. 16, no. 4, pp. 687–693. doi: 10.1109/61.956757.

[45] G. Liu, F. Xu, and Y. Zhou, "Optimized coordinated control strategy of assembly HVDC breakers for MMC based HVDC grids," in *Proc. Int. Conf. Power Syst. Technol.*, 2018, pp. 221–229.

[46] L. Liu, S. Liu, M. Popov, "Optimized algorithm of active injection circuit to calibrate DC circuit breaker,"

Int. J. Electr. Power Energy Syst., vol. 103, pp. 369–376, 2018. doi: 10.1016/j.ijepes.2018.05.020.

[47] B. Xu, R. Ding, J. Zhang, L. Sha, and M. Cheng, "Multiphysics coupled modeling: Simulation of hydraulic operating mechanism for SF6 high voltage circuit breaker," *IEEE/ASME Trans. Mechatronics*, vol. 21, no. 1, pp. 379–393, 2015. doi: 10.1109/TMECH.2015.2460351.

[48] W. Liu, F. Liu, X. Zha, M. Huang, C. Chen, and Y. Zhuang, "An improved SSCB combining fault interruption and fault location functions for DC line short circuit fault protection," *IEEE Trans. Power Del.*, vol. 34, no. 3, pp. 858–868, 2019. doi: 10.1109/TPWRD.2018.2882497.

[49] L. Ängquist, A. Baudoin, T. Modeer, S. Nee and S. Norrga, "VARC – A cost-effective ultra-fast dc circuit breaker concept," in *Proc. IEEE Power & Energy Soc. General Meeting (PESGM)*, Portland, OR, 2018, pp. 1–5. doi: 10.1109/PESGM.2018.8586299.

[50] S. Liu et al., "Modelling, experimental validation and application of VARC HVDC circuit breakers," *IEEE Trans. Power Del.*, vol. 35, no. 3, pp. 1515–1526, 2020. doi: 10.1109/TPWRD.2019.2947544.

[51] A. Hassanpoor, J. Hafner, and B. Jacobson, "Technical assessment of load commutation switch in hybrid HVDC breaker," *IEEE Trans. Power Electron.*, vol. 30, no. 10, pp. 5393–5400, 2015. doi: 10.1109/TPEL.2014.2372815.

[52] W. Wen et al., "Research on a current commutation drive circuit for hybrid dc circuit breaker and its optimisation design," *IET Gener., Transmiss. Distrib.*, vol. 10, no. 13, pp. 3119–3126, 2016. doi: 10.1049/iet-gtd.2015.0840.

[53] J. A. Corea-Araujo, J. A. Martinez-Velasco, and J. Magnusson, "Optimum design of hybrid HVDC circuit breakers using a parallel genetic algorithm and a MATLAB-EMTP environment," *IET Generat., Transmiss. Distrib.*, 2017. vol. 11, no. 12, pp. 2974–2982. doi: 10.1049/iet-gtd.2016.1500.

[54] S. Wang, Z. Song, P. Fu, K. Wang, et al., "Thermal analysis of water-cooled heat sink for solid-state circuit breaker based on IGCTs in parallel," *IEEE Trans. Compon. Packag. Manuf. Technol.*, vol. 9, no. 3, pp. 483–488, doi: 10.1109/TCPMT.2018.2868049.

[55] L. Mackey, C. Peng, and I. Husain, "Progressive switching of hybrid DC circuit breakers for faster fault isolation," in *Proc. IEEE Energy Conversion Congr. Expo. (ECCE)*, 2018, pp. 7150–7157.

[56] B. Yang et al., "A novel commutation-based hybrid HVDC circuit breaker," in *Proc. CIGRÉ Winnipeg Colloq.*, Canada, Oct. 2017, pp. 1–6.

[57] W. Liu, F. Liu, Y. Zhuang, X. Zha, C. Chen, and T. Yu, "A multiport circuit breaker-based multiterminal DC system fault protection," *IEEE J. Emerg. Select. Topics Power Electron.*, vol. 7, no. 1, pp. 118–127, 2019. doi: 10.1109/JESTPE.2018.2885547.

[58] W. Liu, F. Liu, X. Zha, C. Chen, and T. Yu, "A topology of the multi-port DC circuit breaker for multi-terminal DC system fault protection," in *Proc. IEEE Energy Conversion Congr. Expo. (ECCE)*, 2017, pp. 3760–3763.

[59] F. Zhang, Y. Ren, Z. Shi, X. Yang, and W. Chen, "Novel hybrid DC circuit breaker based on series connection of thyristors and IGBT half-bridge submodules," *IEEE Trans. Power Electron.*, vol. 36, no. 2, pp. 1506–1518, 2021. doi: 10.1109/TPEL.2020.3010965.

[60] J. Zhu, X. Guo, J. Yin, Q. Huo, and T. Wei, "Basic topology, modeling and evaluation of a novel hybrid DC breaker for HVDC grid," *IEEE Trans. Power Del.*, early access, Oct. 16, 2021.

[61] T. Augustin, M. Becerra, and H. Nee, "Enhanced active resonant DC circuit breakers based on discharge closing switches," *IEEE Trans. Power Del.*, vol. 36, no. 3, pp. 1735–1743, 2021. doi: 10.1109/TPWRD.2020.3014084.

[62] Y. Guo, G. Wang, D. Zeng, H. Li, and H. Chao, "A thyristor full-bridge-based DC circuit breaker," *IEEE Trans. Power Electron.*, vol. 35, no. 1, 2020, pp. 1111–1123, doi: 10.1109/TPEL.2019.2915808.

[63] S. Wang, C. E. Ugalde-Loo, C. Li, J. Liang, and O. D. Adeuyi, "Bridge-type integrated hybrid DC circuit breakers," *IEEE J. Emerg. Select. Topics Power Electron.*, vol. 8, no. 2, pp. 1134–1151, 2020. doi: 10.1109/JESTPE.2019.2900492.

[64] J. He et al., "A high-performance and economical multiport hybrid direct current circuit breaker," *IEEE Trans. Ind. Electron.*, vol. 67, no. 10, pp. 8921–8930, 2020. doi: 10.1109/TIE.2019.2947835.

[65] S. Wang, W. Ming, W. Liu, C. Li, C. E. Ugalde Loo, and J. Liang, "A multi-function integrated circuit breaker for DC grid applications," *IEEE Trans. Power Del.*, vol. 36, no. 2, pp. 566–577, 2021.

[66] O. Cwikowski et al., "Integrated HVDC circuit breakers with current flow control capability," *IEEE Trans. Power Del.*, vol. 33, no. 1, pp. 371–380, 2018. doi: 10.1109/TPWRD.2017.2711963.

[67] E. Veilleux and B. Ooi, "Multiterminal HVDC with thyristor power-flow controller," *IEEE Trans. Power Del.*, vol. 27, no. 3, pp. 1205–1212, 2012. doi: 10.1109/TPWRD.2012.2187463.

[68] Q. Mu, J. Liang, Y. Li, and X. Zhou, "Power flow control devices in DC grids," *IEEE Power Energy Soc. General Meeting*, San Diego, CA, 2012. pp. 1–7.

[69] C. D. Barker and R. S. Whitehouse, "A current flow controller for use in HVDC grids," in *Proc. 10th IET Int. Conf. AC and DC Power Transmission (ACDC 2012)*, Birmingham, 2012, pp. 1–5. doi: 10.1049/cp.2012.1973.

[70] M. Stumpe, P. Tünnerhoff, J. Dave, A. Schnettler, et al., "DC fault protection for modular multi-level converter-based HVDC multi-terminal systems with solid state circuit breakers," *IET Generation, Transmiss. Distrib.*, vol. 12, no. 12, pp. 3013–3020, 2018. doi: 10.1049/iet-gtd.2017.1322.

[71] S. Liu, Z. Liu, J. de Jesus Chavez, and M. Popov, "Mechanical DC circuit breaker model for real time simulations," *Int. J. Electr. Power Energy Syst.*, vol. 107, pp. 110–119, May 2019. doi: 10.1016/j.ijepes.2018.11.014.

[72] S. S. Mirhosseini, S. Liu, J. C. Muro, Z. Liu, S. Jamali, and M. Popov, "Modeling a voltage source converter assisted resonant current DC breaker for real time studies," *Int. J. Electr. Power Energy Syst.*, vol. 117, p. 117, 2020. doi: 10.1016/j.ijepes.2019.105678.

[73] S. Wang, C. Li, O. D. Adeuyi, G. Li, C. E. Ugalde-Loo, and J. Liang, "Coordination of MMCs with hybrid DC circuit breakers for HVDC grid protection," *IEEE Trans. Power Del.*, 2019. vol. 34, no. 1, pp. 11–22, doi: 10.1109/TPWRD.2018.2828705.

[74] H. Xiao, Z. Xu, L. Xiao, C. Gan, F. Xu, and L. Dai, "Components sharing based integrated HVDC circuit breaker for meshed HVDC grids," *IEEE Trans. Power Del.*, vol. 35, no. 4, pp. 1856–1866, Aug. 2020. doi: 10.1109/TPWRD.2019.2955726.

[75] C. Meyer, M. Kowal and R. W. De Doncker, "Circuit breaker concepts for future high-power DC-applications," in *Proc. 14th IAS Annu. Meeting Conf. Rec. 2005 Ind. Appl. Conf.*, 2005, Kowloon, Hong Kong, 2005, pp. 860–866.

[76] B. Mitra and B. Chowdhury, "Comparative analysis of hybrid DC breaker and assembly HVDC breaker," in *Proc. North Amer. Power Symp.*, Morgantown, WV, 2017, pp. 1–6.

[77] T. Schultz, V. Lenz and C. M. Franck, "Circuit breakers for fault current interruption in HVDC grids," in *VDE High Voltage Technol. 2016; ETG-Symp.*, Berlin, Deutschland, 2016, pp. 1–6.

[78] T. U. Derakhshanfar, U. Jonsson, Steiger, and M. Habert, "Hybrid HVDC breaker – A solution for future HVDC system," in *Proc. CIGRE 2014*, Paris, France, 2014.

[79] M. Rahimo et al., "The Bimode Insulated Gate Transistor (BIGT), an ideal power semiconductor for power electronics based DC Breaker applications," *CIGRE Parsis Session*, 2014, p. B4-302.

[80] Alibaba Global Direct Sourcing Platform. VEI-KAI vacuum interrupter VK12-40.5P. [Online]. Available: https://www.alibaba.com/product-detail/VK12-40-5P-40-5KV-31_62464937198.html?spm=a2700.7724857.normalList.57.7e504b81SrdmYr

[81] F. Xu, Y. Lu, X. Ni and C. Wang, "A low-cost multi-port type HVDC breaker for HVDC grids," in *Proc. IEEE Int. Conf. Energ. Internet (ICEI)*, Nanjing, China, 2019, pp. 121–126. doi: 10.1109/ICEI.2019.00028.

[82] S. Zhang, G. Zou, X. Wei, and C. Sun, "Diode-bridge multi-port hybrid DC circuit breaker for multi-terminal DC grids," *IEEE Trans. Ind. Electron.*, vol. 68, no. 1, pp. 270–281, 2021.

[83] G. P. Ased et al., "Continued operation of multi-terminal HVDC networks based on modular multilevel converters," in *Proc. CIGRÉ Int. Symp.*, 2015, pp. 1–8.

[84] S. Yang, W. Xiang, X. Lu, W. Zuo, and J. Wen, "An adaptive reclosing strategy for MMC-HVDC systems with hybrid DC circuit breakers," *IEEE Trans. Power Del.*, vol. 35, no. 3, pp. 1111–1123, 2019. doi: 10.1109/TPWRD.2019.2935311.

[85] T. Wang, G. Song, and K. S. T. Hussain, "Adaptive single-pole auto-reclosing scheme for hybrid MMC-HVDC systems breakers," *IEEE Trans. Power Del.*, vol. 34, no. 6, pp. 2194–2203, 2019. doi: 10.1109/TPWRD.2019.2921674.

[86] B. Li, H. Cui, B. Li, W. Wen, and D. Dai, "A permanent fault identification method for single-pole grounding fault of overhead transmission lines in VSC-HVDC grid based on fault line voltage," *Int. J. Electr. Power Energy Syst.*, vol. 117, p. 105,603, 2020. doi: 10.1016/j.ijepes.2019.105603.

[87] B. Li, J. He, Y. Li, and W. Wen, "A novel DCCB reclosing strategy for the flexible HVDC grid breakers," *IEEE Trans. Power Del.*, vol. 35, no. 1, pp. 244–257, 2020. doi: 10.1109/TPWRD.2019.2938594.

[88] X. Fan and B. Zhang, "DC line soft reclosing sequence for HVDC grid based on hybrid DC breaker," *J. Eng.*, vol. 2019, no. 16, pp. 1095–1099, 2019. doi: 10.1049/joe.2018.8432.

[89] P. E. I. Xiangyu, T. A. N. G. Guangfu, and S. Zhang, "Sequential auto-reclosing strategy for hybrid HVDC breakers in VSC-based DC grids," *J. Modern Power Syst. Clean Energ.*, vol. 7, no. 3, pp. 633–643, 2019. doi: 10.1007/s40565-018-0486-1.

[90] M. Cheah-Mane, O. D. Adeuyi, J. Liang and N. Jenkins, "A scaling method for a multi-terminal DC experimental test rig," in *Proc. 17th European Conf. Power Electron. Appl. (EPE'15 ECCE-Europe)*, Geneva, Switzerland, 2015, pp. 1–9.

[91] A. Shemshadi, "Modeling of plasma dispersion process in vacuum interrupters during postarc interval based on FEM," *IEEE Trans. Plasma Sci.*, vol. 47, no. 1, pp. 647–653, 2019. doi: 10.1109/TPS.2018.2879519.

[92] G. Li, J. Liang, S. Balasubramaniam, T. Joseph, and D. Kong, "Experimental validation of DC circuit-breakers for MTDC grid protection," in *Proc. 15th IET Int. Conf. AC and DC Power Transmission (ACDC 2019)*, Coventry, U.K., 2019, pp. 1–6.

[93] O. N. Cwikowski, "Synthetic testing of high voltage direct current circuit breakers," PhD thesis, Univ. of Manchester, 2016.

[94] D. Liang, X. Guo, Y. Gao, and J. Zou, et al., "Investigations on a new synthetic test of dc vacuum circuit breaker," in *Proc. IEEE 3rd Adv. Inf. Technol., Electron. Automat. Control Conf. (IAEAC)*, 2018, pp. 1376–1379.

[95] N. A. Belda and R. P. P. Smeets, "Test circuits for HVDC circuit breakers," *IEEE Trans. Power Del.*, vol. 32, no. 1, pp. 285–293, 2017. doi: 10.1109/TPWRD.2016.2567783.

[96] N. A. Belda, C. A. Plet, and R. P. P. Smeets, "Full-power test of HVDC circuit-breakers with AC short-circuit generators operated at low power frequency," *IEEE Trans. Power Del.*, vol. 34, no. 5, pp. 1843–1852, 2019. doi: 10.1109/TPWRD.2019.2910141.

[97] X. Han, W. Sima, M. Yang, L. Li, T. Yuan, and Y. Si, "Transient characteristics under ground and short-circuit faults in a MMC-based HVDC system with hybrid DC circuit breakers," *IEEE Trans. Power Del.*, vol. 33, no. 3, pp. 1378–1387, 2018. doi: 10.1109/TPWRD.2018.2795800.